Fetuin B alleviates testosterone propionate-induced oxidative stress and mitochondrial dysfunction in KGN cells by upregulating the TGFR2/SMAD3 pathway

Yiyin Gao
The Second Hospital of Jilin University
Lianwen Zheng
The Second Hospital of Jilin University
Guijie Wu
The Second Hospital of Jilin University
Yalan Ma
Affiliated Hospital of Jining Medical University
Yinggang Zou (zouyg@jlu.edu.cn)
The Second Hospital of Jilin University

Research Article

Keywords: polycystic ovary syndrome, FETUB, proteomics, oxidative stress, granulosa cells

Posted Date: September 15th, 2022

DOI: https://doi.org/10.21203/rs.3.rs-2048203/v1

Abstract

Background

Polycystic ovary syndrome (PCOS) is one of the most common reproduction and endocrine disorders. Patients with abnormal follicle growth develop ovulation disorders and amenorrhea, and eventually infertility. The role of Fetuin-B (FETUB), one of the differentially expressed proteins (DEPs) in follicular fluid (FF) of PCOS patients, in pathogenesis of PCOS was not clearly clarified.

Methods

In this study, we performed iTRAQ-based quantitative proteomic analysis on FF collected from non-PCOS healthy controls and PCOS patients to identify DEPs. In addition, KGN cells treated with testosterone propionate (TP) were used as a model of hyperandrogenism in vitro to investigate the regulatory effects of the selected DEP, FETUB, on cellular processes in KGN cells and its molecular mechanism by detecting steroid hormone secretion, measuring indicators of oxidative stress (OS), mitochondria functions and apoptosis and characterizing the FETUB-altered downstream signaling.

Results

We found that supplementation with recombinant FETUB could significantly restore the total antioxidant capacity and activity of antioxidant enzymes, which were reduced by treatment with TP. Additionally, FETUB restored the secretory and mitochondrial functions in TP-impaired KGN cells and reduced their apoptosis. Furthermore, our study revealed that FETUB could bind with transforming growth factor beta receptor 2 (TGFR2) on the cell membrane of KGN cells and promote phosphorylation of SMAD3, which had a therapeutic effect against tissue injury and inflammation. And the protective effect of FETUB on TP-treated KGN cells was inhibited by pre-treatment with SB431542 and SIS3, selective inhibitors of TGFR2 and SMAD3, respectively.

Conclusions

These results indicate that FETUB may protect TP-treated KGN by alleviating OS and mitochondrial dysfunction via the TGFR2-mediated SMAD pathway.

Data are available via ProteomeXchange with identifier PXD036531

Background

Polycystic ovary syndrome (PCOS) is a common reproductive endocrine disorder that affects about 5–15% of women of reproductive age worldwide[1, 2]. The pathophysiology of PCOS often involves a variety

of metabolic and endocrine diseases, showing a variety of symptoms, such as hyperandrogenism, insulin resistance, ovulatory dysfunction, and gonadotropin (GN) disorders[3]. Although the exact pathogenesis of PCOS remains unknown, it is generally thought to be related to oxidative stress (OS), chronic low-grade inflammation, and mitochondrial dysfunction, which have an adverse effect ovarian function and ultimately lead to reduced female fertility[4, 5]. Follicular fluid (FF) is rich in cytokines secreted by granulosa cells (GCs), which can regulate ovarian function and promote follicular growth and oocyte maturation. Therefore, elucidating the protein composition of FF is crucial to understand the function of ovarian GCs and the process of follicular growth and development[6].

Fetuin B (FETUB), a member of the fetuin protein family part of the cystatin superfamily of cysteine protease inhibitors, has been implicated in regulating physiological or pathophysiological processes, including fertility, energy metabolism, and liver disease. Fetuin A (FETUA), which is 22% homologous to FETUB, can trigger the insulin resistance (IR) by activating Toll-like receptors and inducing inflammation [7]. However, unlike FETUA, the physiological concentration of FETUB does not induce proinflammatory signaling[8]. Although an independent association between serum FETUB and IR has been reported in women with PCOS, with significantly lower concentration of FETUB after improvement of the IR[9]. In addition, the FETUB mRNA level was downregulated in the acute phase of inflammation in rats, which indicated that it might have a crucial role in the recovery from the acute phase of the inflammation[10]. However, as an acute-phase reactive protein, changes in FETUB expression in acute-phase inflammation are significantly different among different species.

In conclusion, we identified differentially expressed proteins (DEPs) in the FF obtained from overweight/obese PCOS group patients and control (CON) group subjects using iTRAQ-based quantitative proteomics. Both the results from the iTRAQ quantitative proteomics analysis and their verification by enzyme-linked immunosorbent assay (ELISA) showed that the level of FETUB secreted into the FF of PCOS patients was significantly higher than that of CON group subjects, suggesting that it may function as a positive acute-phase response protein in humans, but its role in PCOS remains unknown. We further investigated the regulatory effects and mechanisms of FETUB on the function of hyperandrogenism-induced GCs *in vitro*. The insights gained from these findings could lay the foundation for future PCOS treatment.

Methods

Patient and Subject Enrollment and Sample Collection

This study enrolled infertile women with and without PCOS seeking assisted reproductive treatment (ART) at the Reproductive Center of Second Hospital of Jilin University between September 2020 and January 2021. All participants were 25-35 years of age and overweight or obese (BMI>23.9 kg/m2). The diagnosis of the 27 women enrolled in the PCOS group was performed according to the Rotterdam criteria, while another 27 infertile women with normal ovarian reserve in the CON group were selected for tubal or male factors. All included patients were treated with the classic long regimen of GN-releasing hormone agonist

for controlled ovarian stimulation. Also, patients with diabetes, cancers, systemic inflammatory diseases, or other diseases that may affect follicular development were excluded from both groups.

FF samples for proteomics analysis were collected from 9 PCOS patients and 9 CON group subjects and pooled randomly to obtain three samples in each of the two groups, while the other FF samples were used for validation of DEPs by ELISA. After 34 to 36 hours of administering 10,000 IU of recombinant human chorionic GN, the FF was aspirated transvaginally under ultrasound guidance. The FF samples with obvious blood contamination were excluded from the analysis. Cells and insoluble particles were removed from the FF samples by centrifugation at 1,000 g for 15 minutes at 4 °C. After separation, the supernatant was stored at 80°C for subsequent use.

Protein Extraction and Quantification in FF

After thawing, FF samples were centrifuged at 12,000 g for 10 minutes at 4°C to eliminate any potential cellular debris. After thoroughly mixing each sample with 1 mM phenylmethylsulfonyl fluoride (PMSF), a 100% trichloroacetic acid (TCA) solution was added dropwise and mixed well. Afterwards, an equal volume of chloroform was added, and the solution was mixed well. After precipitation on ice for 1 hour, the samples were centrifuged at 1,500 g for 10 minutes, and the supernatant was separated, and the pH was adjusted to 2-3 with 1 M tetraethylammonium bromide (TEAB). Highly abundant proteins were removed using the ProteoMiner Protein Enrichment Kit (Bio-Rad Laboratories Inc., Hercules, CA, USA). Additionally, protein concentration was determined using a Bradford Protein Assay Kit (Beyotime Biotechnology Co., Ltd., Shanghai, China).

Enzymatic Digestion and Desalting

Protein (100 μg) was dissolved to a concentration of about 1 μg/μL with U2 lysis buffer (8 M Urea, 10 mM EDTA) and diluted 6-fold with TEAB. Protein was then digested by incubation overnight at 37°C with trypsin in an appropriate ratio. The ratio of peptide sample to C18 column material was 1000:1. After activating the column material with methanol, it was centrifuge with shaking. The precipitate was acidified by adding 1 mL of 0.1% formic acid (FA), centrifuged again and the supernatant was discarded. After acidification, peptide samples were vortexed, mixed by stirring for 30 minutes and then centrifuged to remove the supernatant. Following two rinses with 0.1 % FA + 3% acetonitrile (ACN) for desalting, the sample was eluted with 0.1 % FA + 80 % ACN. The eluted peptide samples were dried in a vacuum concentrator.

iTRAQ Labeling and Fractionation

The peptide sample was dissolved in 0.5 M TEAB and isopropanol and then centrifuged. Samples were labeled using the iTRAQ Reagent-8 plex Multiplex Kit (AB Sciex U.K. Limited, Warrington, UK) according to

the manufacturer's instructions, and designated by numbers ranging from 113 to 118. A Thermo Dionex UltiMate™ 3000 BioRS high-performance liquid chromatography (HPLC) system (Thermo Fisher Scientific Inc., Waltham, MA, USA) equipped with a Welch C18 column (5 μm, 100 Å, 4.6×250 mm) was used at high pH to fractionate all of the labeled samples in an equal proportion. Ultimately, the 12 collected fractions were mixed, desalted on a Strata-X column and vacuum-dried.

Liquid Chromatography Tandem Mass Spectrometry (LC-MS/MS) Analysis

On-board buffer was used to dilute peptide samples with sample volume of 8 μl and a scanning mode of 90 minutes. Peptides with a mass-to-charge ratio of 350–1,200 were identified and analyzed using the Triple time-of-flight (TOF) 5600+ mass spectrometer System coupled with the Eksigent nanoLC System (AB Sciex, Framingham, MA, USA),. After loading onto a C18 trap column (3μm, 350 μm×50 mm), the peptides were eluted at 300 nL/min over a 90-minute gradient onto an analytical column (3 μm, 75 μm×150 mm). Buffers A and B, which contained 2% ACN/0.1% FA/98% H_2O and 98% ACN/0.1% FA/2% H_2O, respectively, were used as the two mobile phases. For information dependent data collection, panoramic scans were collected in 250 ms and 40 production scans were acquired in 50 ms. The m/z scan range was set at 350-1,500 for MS1 spectra and 100-1,500 for MS2 spectra. The precursor ion dynamic exclusion time was set to 15 s.

Database Search

The ProteoPilot 4.5 software (July 2012; AB Sciex) was used to search and analyze the database of the MS off-board data. The retrieval parameters were set as listed in Table 1. The geometric mean of the ratios of all replicates from the two groups of samples was calculated, and the p-value of all comparison groups output by the ProteinPilot software was used to calculate the significance of the difference using the z-score test to obtain the overall significance p-value of the comparison between groups. After the statistical test, the adj.*P*-value of the comparison group was less than or equal to 0.05, and when the fold change between the two groups was 1.2 fold or more, or less than 0.83 fold, the protein was considered as a DEP between the two groups.

Table 1 Parameters of searching in ProteinPilot database

Parameters	Setting
Type of search	iTRAQ 8plex (Peptide Labeled)
Enzyme	Trypsin
Cys Alkylation	Iodoacetamide
Instrument	TripleTOF 5600
Bias Correction	TRUE
Background Correction	TRUE
ID focus	Biological modifications
Search Effort	Thorough ID
Protein Mass	Unrestricted
Database	See in Report

ELISA Validation

ELISA was used to further validate four chosen DEPs using FF samples from an additional 36 participants, including lipoprotein lipase (LPL), quiescin sulfhydryl oxidase 1 (QSOX1), FETUB, and afamin (AFM). For the LPL, QSOX1, FETUB, and AFM assay, the samples were diluted to a concentration of 1:200, 1:1, 1:100, and 1:100, respectively, followed by the measurement of their concentration with commercial ELISA kits (CUSABIO, Wuhan, China).

Treatment of KGN cells

The human ovarian granulosa cell line KGN used in this study was cultured in Dulbecco's modified Eagle's medium (DMEM) containing 10% fetal bovine serum (FBS), 100 U/mL penicillin and 100 μg/mL streptomycin in a cell culture incubator at 37°C with 5% CO_2. All experiments were performed with cells at passage 3–10 at 70% confluence and starved for 12 hours in DMEM without FBS.

KGN cells were grown in the presence (50 ng/mL) or absence of recombinant FETUB (Abnova Corporation, Taipei City, Taiwan, China) for 4 hours before exposure to 50 μM TP for 12 hours. In addition, after pretreatment with 10 nM SB431542 (MedChemExpress (MCE), Monmouth Junction, NJ, USA), 3 mM SIS3 (MCE) or 10 mM ML385 (MCE) for 1 hour, 50 ng/mL FETUB were added for 4 hours, followed by stimulation with 50 μM TP for 12 hours.

Measurement of Reactive Oxygen Species (ROS), O_2^- and Mitochondrial Superoxide Levels

KGN cells were treated as described above. Then, according to the instructions of the different dye kits, KGN cells were incubated for 25 minutes with dichloro-dihydro-fluorescein diacetate (DCFH-DA) from a Reactive Oxygen Species Assay Kit (Beyotime Biotechnology Co., Ltd.), or for 30 minutes with dihydroethidium (DHE, Beyotime Biotechnology Co., Ltd.) or for 10 minutes with MitoSOX Red indicator (Invitrogen, Carlsbad, CA, USA) in the dark at 37 ℃. Flow cytometry was used to detect the level of intracellular ROS, O_2^- and mitochondrial superoxide.

Measurement of Pro- and Antioxidant-related Variables

KGN cells were treated as described above. After preparing the protein samples extracted from cells, the contents of malondialdehyde (MDA) and reduced glutathione (GSH) were determined with the Lipid Peroxidation MDA Assay Kit (Beyotime Biotechnology Co., Ltd.) and GSH and GSSG Assay Kit (Beyotime Biotechnology Co., Ltd.). In addition, the activity of antioxidant enzymes, such as superoxide dismutase (SOD), catalase (CAT), glutathione peroxidase (GPx) and glutathione reductase (GR) was measured using the corresponding assay kit (Beyotime Biotechnology Co., Ltd.).

Measurement of Mitochondrial Membrane Potential (MMP) and ATP Level

KGN cells were treated as described above. The MMP of KGN cells was measured by both flow cytometry and fluorescence microscopy with JC-1 solution (Beyotime Biotechnology Co., Ltd.) and tetramethylrhodamine ethyl ester (TMRE) fluorescent dye (Beyotime Biotechnology Co., Ltd.) and Hoechst 33342 dye (Thermo Fisher Scientific Inc.). The ATP content was measured using the Enhanced ATP Detection Kit (Beyotime Biotechnology Co., Ltd.) according to the manufacturer's instructions.

Measurement of hormones secretion

KGN cells were treated as described above. The levels of estradiol (E_2) and progesterone (P) were determined in collected supernatants of cell culture medium using ELISA kits (CUSABIO).

Cell apoptosis analysis

KGN cells were treated as described above. Cell apoptosis was measured after staining cells by incubation for 20 minutes with annexin V-fluorescein isothiocyanate (FITC) and propidium iodide (PI)

(Beyotime Biotechnology). FITC-Annexin V positive apoptotic cells were identified by flow cytometry. A *CASP3*(caspase 3) Activity Assay Kit (Beyotime Biotechnology Co., Ltd.) was used to measure CASP3 activity.

Quantitative Reverse Transcription-Polymerase Chain Reaction (qRT-PCR)

Total RNA was isolated from cells using the TriPure Isolation Reagent (Merck KGaA, Darmstadt, Germany) following the manufacturer's instructions. The PrimeScriptTM RT Master Mix (Takara Bio, Shiga, Japan) was used to reverse transcribe total RNAs into cDNAs. The qRT-PCR analysis was performed using the FastStart Universal SYBR Green Master (Rox) Mix (Roche Diagnostics GmbH, Basel, Switzerland).

The mRNA expression level was determined by measuring the cycle threshold (Ct) value and normalizing it against the Ct value of the reference gene glyceraldehyde-3-phosphate dehydrogenase (*GAPDH*). The $2^{-\Delta\Delta Ct}$ approach was used to obtain the values for relative quantification as fold-change in comparison to the CON group[11]. The sequences of the primers for related genes are shown in Table 2.

Table 2 Primer sequence of related gene

Gene Name	Primer Sequences 5'→3'
STAR	F:CAGACTTCGGGAACATGCCT
	R:GGGACAGGACCTGGTTGATG
CYP11A1	F:CCCTGTTGGATGCAGTGTCT
CYP19A1	R:TTGAGCACAGGGTACTTTA
	F:GGACCCCTCATCTCCCACG
	R:CCCAAGTTTGCTGCCGAAT
HSD3B1	F:AGCATCCGAGGACAGTTCTAC
BCL2	R:AGGGCGGTCGATAGGTGTAA
BAX	F:GCCGGTTCAGGTACTCAGTC
CASP3	R:GCCGGTTCAGGTACTCAGTC
GAPDH	F:ACGGCCTCCTCTCCTACTTT
	R:GCCTCAGCCCATCTTCTTC
	F:CTGGACTGTGGCATTGAGAC
	R:GCAAAGGGACTGGATGAACC
	F:ATTTGGCTACAGCAACAGG
	R:TTGAGCACAGGGTACTTTATT

Steroidogenic acute regulatory protein (*STAR*), cytochrome P450 family 11 subfamily a member 1 (*CYP11A1*), hydroxy-delta-5-steroid dehydrogenase, 3b-hydroxysteroid dehydrogenase (*HSD3B1*), cytochrome P450 family 19 subfamily a member 1 (*CYP19A1*).

Membrane Protein Extraction and Immunoprecipitation

Plasma membrane protein from KGN cells was extracted using the Plasma Membrane Protein Extraction kit (Abcam, Cambridge, UK) as directed by the manufacturer. The isolated plasma membrane proteins were incubated with 5 μg of an anti-FETUB antibody (Santa Cruz Biotechnology, Santa Cruz, CA, USA) overnight at 4 ℃. The immunocomplex was incubated with protein A/G beads for 1 hour at room temperature for precipitation. Beads were washed twice with Immunoprecipitation (IP) Lysis/Wash Buffer of the Pierce Co-Immunoprecipitation (Co-IP) Kit (Thermo Fisher Scientific Inc.) and once with pure water, followed by elution in the lane marker sample buffer. Subsequently, protein samples were collected and immunoblotted with anti-FETUB or anti-TGFR2 (Abcam) antibodies.

Western Blot Analysis

Proteins were extracted from KGN cells, resolved by sodium dodecyl sulfate-polyacrylamide gel electrophoresis (SDS-PAGE) and transferred to polyvinylidene difluoride (PVDF) membranes (Millipore Sigma, Burlington, MA, USA). Then, membranes with transferred proteins were incubated with primary antibodies overnight at 4 °C. Afterwards, membranes were incubated for 1 hour with appropriate anti-rabbit or anti-mouse IgG secondary antibodies (Proteintech Group Inc., Rosemont, IL, USA), and immunoreacted proteins were visualized by the chemiluminescence method (Proteintech Group Inc.).

Antibodies against pSMAD3 (9520S, dilution: 1:1,000) were obtained from Cell Signaling Technology (Danvers, MA, USA). Antibodies against β-actin (60008, dilution: 1:2,500) were obtained from Proteintech Group Inc. Western blot immunoreacted protein bands were quantified using the Image J software (National Institute of Health (NIH), Bethesda, MD, USA).

Statistical analysis

All experiments were performed three times independently. One-way analysis of variance (ANOVA) was used to determine whether the data difference between various groups were statistically significant using the SPSS 26.0 software (IBM Corporation, Armonk, NY, USA). The graphs of the experimental results were plotted with the GraphPad Prism 8.0 software (GraphPad Software Inc., San Diego, USA), and $P<0.05$ was considered statistically significant.

Results

Comparison of general clinical data and pregnancy outcome parameters of study subjects

As shown in Table 3, most of parameters reflecting ovarian reserve function were different between PCOS and CON group. The serum basal LH level, LH/FSH ratio, basal E_2 level, basal T level and basal antral follicle number in the PCOS group were all significantly higher than those in the CON group, while other parameters reflecting the basic condition showed no significant differences, such as age, body-mass index (BMI), infertility duration and basal serum follicle-stimulating hormone (FSH) ($P > 0.05$). At the same time, the comparison of ovarian reactivity-related parameters, such as endometrial thickness on trigger day, and level of hormone on trigger day, were not statistically different between the PCOS and CON groups ($P > 0.05$). Regarding the pregnancy outcome parameters, the mature oocytes rate and fertilization rate in the PCOS group was significantly lower than that in the CON group. In addition, there was no statistical difference in the clinical pregnancy rate ($P > 0.05$).

Table 3
Comparison of Clinical characters and pregnancy outcomes bewteen participants in PCOS & CON groups(± S)

Parameters	PCOS group (N = 27)	CON group (N = 27)	*P*
Age (year)	30.85 ± 2.96	30.70 ± 3.31	0.863
BMI (Kg/m2)	28.20 ± 3.30	26.98 ± 2.16	0.113
Years of infertility (year)	4.65 ± 3.39	3.46 ± 2.19	0.133
Basal FSH (mIU/mL)	4.85 ± 4.25	6.83 ± 3.24	0.059
Basal LH (mIU/mL)	5.22 ± 3.01	3.57 ± 1.57	0.015*
LH/FSH ratio	1.40 ± 0.63	0.55 ± 0.24	0.000*
Basal E_2 (pg/mL)	53.28 ± 30.02	39.24 ± 11.29	0.027*
Basal T (ng/mL)	0.93 ± 0.35	0.43 ± 0.14	0.000*
Basal number of antral follicles	22.00 ± 5.73	15.70 ± 2.64	0.000*
No. of follicles > 18mm on trigger day	8.81 ± 3.43	8.22 ± 2.03	0.443
Thickness of endometrium on trigger day (mm)	9.93 ± 2.43	10.22 ± 2.08	0.639
LH level on trigger day (mIU/mL)	2.96 ± 3.13	1.56 ± 1.00	0.031*
P level on trigger day (ng/mL)	1.09 ± 0.57	0.88 ± 0.51	0.144
E_2 level on trigger day (pg/mL)	2580.35 ± 2188.75	1883.83 ± 1233.12	0.156
No. of retrieved oocytes	10.52 ± 4.58	9.11 ± 1.99	0.149
Proportion of mature oocytes	65.49% (186/284)	79.27% (195/246)	0.000*
Rate of fertilization	61.27% (174/284)	73.98% (182/246)	0.002*
Proportion of transferable embryos	63.22% (110/174)	87.91% (130/182)	0.099
Rate of clinical pregnancy	44.44% (12/27)	55.55% (15/27)	0.414

Results are presented as mean ± standard deviation. BMI, body mass index; FSH, follicle-stimulating hormone; LH, luteinizing hormone; E2, estradiol; T, testosterone.

Quantitative MS Analysis of FF

The comparison of the overall proteome profiling of FF from the PCOS and CON groups determined by quantitative proteomic analysis on pooled FF samples qualitatively identified 586 proteins and 7,970 peptides in total from two groups. Among them, there were 68 DEPs between the two groups, including 28

upregulated DEPs and 39 downregulated DEPs in the PCOS group. The accession number, name, fold change and P value of the various proteins are shown in Table 4. A heat map generated by unsupervised hierarchical clustering was used to show the changes in the levels of DEPs in each of the pooled samples (Fig. 1A).

Table 4
List of DEPs detected in FF by proteomics between PCOS and CON group

Accession	Name	Fold change	P-value
O75636	Ficolin-3 GN = FCN3	5.288	0.042
A0A0C4D	Immunoglobulin kappa variable 3D-20 GN = IGKV3D-20	4.878	0.023
P08697	Alpha-2-antiplasmin GN = SERPINF2	3.875	0.045
P03952	Plasma kallikrein GN = KLKB1	3.088	0.001
Q14520	Hyaluronan-binding protein 2 GN = HABP2	3.049	0.018
Q9UGM5	Fetuin-B GN = FETUB	2.978	0.035
Q6UWH4	Golgi-associated kinase 1B GN = GASK1B	2.867	0.015
P01591	Immunoglobulin J chain GN = JCHAIN	2.809	0.007
P00748	Coagulation factor XII GN = F12	2.477	0.003
Q08830	Fibrinogen-like protein 1 GN = FGL1	2.424	0.011
Q92954	Proteoglycan 4 GN = PRG4	2.401	0.014
P01871	Immunoglobulin heavy constant mu GN = IGHM	2.256	0.023
Q16610	Extracellular matrix protein 1 GN = ECM1	2.212	0.036
P06858	Lipoprotein lipase GN = LPL	2.131	0.002
O43866	CD5 antigen-like GN = CD5L	2.067	0.015
Q9UBQ6	Exostosin-like 2 GN = EXTL2	2.016	0.014
P05111	Inhibin alpha chain GN = INHA	1.926	0.038
P60981	Destrin GN = DSTN	1.808	0.039
Q9GZM7	Tubulointerstitial nephritis antigen-like GN = TINAGL1	1.692	0.021
P06280	Alpha-galactosidase A GN = GLA	1.645	0.007
Q9UBP4	Dickkopf-related protein 3 GN = DKK3	1.616	0.002
Q9H8L6	Multimerin-2 GN = MMRN2	1.577	0.029
P52272	Heterogeneous nuclear ribonucleoprotein M GN = HNRNPM	1.516	0.026
P00739	Haptoglobin-related protein GN = HPR	1.485	0.033
Q86UD1	Out at first protein homolog GN = OAF	1.477	0.005
P01824	Immunoglobulin heavy variable 4–39 GN = IGHV4-39	1.436	0.011

Accession	Name	Fold change	P-value
P46778	60S ribosomal protein L21 GN = RPL21	1.414	0.041
P10321	HLA class I histocompatibility antigen C alpha chain GN = HLA-C	1.409	0.033
Q14974	Importin subunit beta-1 GN = KPNB1	1.206	0.041
P13010	X-ray repair cross-complementing protein 5 GN = XRCC5	0.832	0.012
P24158	Myeloblastin GN = PRTN3	0.810	0.045
P17936	Insulin-like growth factor-binding protein 3 GN = IGFBP3	0.800	0.041
P62979	Ubiquitin-40S ribosomal protein S27a GN = RPS27A	0.789	0.043
P05543	Thyroxine-binding globulin GN = SERPINA7	0.753	0.017
P19021	Peptidyl-glycine alpha-amidating monooxygenase GN = PAM	0.716	0.015
P55083	Microfibril-associated glycoprotein 4 GN = MFAP4	0.712	0.014
P14061	Estradiol 17-beta-dehydrogenase 1 GN = HSD17B1	0.710	0.045
Q9UNW1	Multiple inositol polyphosphate phosphatase 1 GN = MINPP1	0.679	0.012
P19652	Alpha-1-acid glycoprotein 2 GN = ORM2	0.673	0.001
P55209	Nucleosome assembly protein 1-like 1 GN = NAP1L1	0.669	0.023
P49327	Fatty acid synthase GN = FASN	0.667	0.041
P48444	Coatomer subunit delta GN = ARCN1	0.626	0.009
Q9NY15	Stabilin-1 GN = STAB1	0.625	0.014
P12268	Inosine-5'-monophosphate dehydrogenase 2 GN = IMPDH2	0.620	0.024
P05121	Plasminogen activator inhibitor 1 GN = SERPINE1	0.615	0.023
P30153	Serine/threonine-protein phosphatase 2A 65 kDa regulatory subunit A alpha isoform GN = PPP2R1A	0.593	0.045
P81605	Dermcidin GN = DCD	0.582	0.031
Q8N2S1	Latent-transforming growth factor beta-binding protein 4 GN = LTBP4	0.568	0.007
Q92743	Serine protease HTRA1 GN = HTRA1	0.557	0.048
P68363	Tubulin alpha-1B chain GN = TUBA1B	0.556	0.033
Q92626	Peroxidasin homolog GN = PXDN	0.551	0.026
P0DMV9	Heat shock 70 kDa protein 1B GN = HSPA1B	0.532	0.042

Accession	Name	Fold change	P-value
P43652	Afamin GN = AFM	0.528	0.011
Q08380	Galectin-3-binding protein GN = LGALS3BP	0.520	0.036
P62258	14-3-3 protein epsilon GN = YWHAE	0.512	0.005
Q92496	Complement factor H-related protein 4 GN = CFHR4	0.504	0.014
P67775	Serine/threonine-protein phosphatase 2A catalytic subunit alpha isoform GN = PPP2CA	0.492	0.036
P15814	Immunoglobulin lambda-like polypeptide 1 GN = IGLL1	0.491	0.018
P08238	Heat shock protein HSP 90-beta GN = HSP90AB1	0.459	0.002
O00391	Quiescin Sulfhydryl oxidase 1 GN = QSOX1	0.452	0.014
Q9Y646	Carboxypeptidase Q GN = CPQ	0.446	0.012
P19012	Keratin type I cytoskeletal 15 GN = KRT15	0.439	0.040
P26373	60S ribosomal protein L13 GN = RPL13	0.426	0.043
P05060	Secretogranin-1 GN = CHGB	0.405	0.023
Q14563	Semaphorin-3A GN = SEMA3A	0.396	0.017
P62701	40S ribosomal protein S4 X isoform GN = RPS4X	0.394	0.037
P68104	Elongation factor 1-alpha 1 GN = EEF1A1	0.393	0.014
P46782	40S ribosomal protein S5 GN = RPS5	0.330	0.036

Functional Enrichment and Clustering Analyses of DEPs

We focused on the DEPs between the two groups to further characterize proteins involved in the progression of PCOS and performed functional annotation and functional enrichment. The results of the gene ontology (GO) term enrichment analysis of the DEPs in PCOS patients revealed that significantly enriched terms associated with genes encoding for the upregulated or downregulated DEPs were related to various processes in the biological process (BP) category of the GO annotation database including cellular processes, metabolic processes, responses to stimuli, immune responses, and other cellular physiological processes. Additionally, significant terms related to the DEPs were associated with components in the cellular component (CC) GO category found in both cellular anatomical entities and protein-containing complexes, as well as with various functions in the molecular function (MF) GO category indicating that higher proportions of DEPs were involved in binding function, catalytic activity, cellular process, metabolic processes, regulation of biological processes, *etc*. (Fig. 1B).

The results of the clusters of orthologous groups (COG) functional classification analysis of the DEPs in the PCOS group showed that the up- and downregulated DEPs between the two groups were all associated with biological activities, such as post-translational modification, lysosomal structure, and biogenesis. In addition, upregulated DEPs were also associated with intracellular transport, secretion, and vesicular transport, while downregulated DEPs were significantly associated lipid transportation and metabolism, as well as energy production and conversion (Fig. 1C).

The top 20 significant pathways identified by Kyoto encyclopedia of genes and genomes (KEGG) pathway enrichment analysis of DEPs are shown in Fig. 1D. The pathways include the following: human-related diseases (*Staphylococcus aureus* infection, primary immune deficiency, autoimmune thyroid disease, *etc*.), biological system related (complement system and blood coagulation cascade activation pathway, antigen processing and presentation process), metabolic related pathway, cellular process related (phagosome, oocyte meiosis), TGF-beta signaling pathway, *etc*.

To further investigate whether there is a significant enrichment trend of DEPs in the PCOS group in certain functional types, we performed GO term and KEGG pathway enrichment analyses of the DEPs (Fig. 2). The GO term enrichment analysis showed that the DEPs were enriched in terms associated with BPs such as those involved in alleviating the oxidation process and regulating the response of cells to growth factor stimulation and were mainly distributed on the membrane of organelles. The results of the KEGG pathway enrichment analysis showed that DEPs were enriched in signaling pathways such as the TGF-beta pathways.

Validation of DEPs by ELISA Analysis

To validate the proteomic results, we selected two upregulated or downregulated DEPs and measured the protein concentration in the FF by ELISA. Among the upregulated DEPs in the FF of PCOS group were FETUB and LPL, whose expression levels were significantly higher in the FF of PCOS patients (Fig. 3A,3B). In contrast, the levels of QSOX1 and AFM in the FF of the PCOS group were significantly lower than those in the CON group, which is consistent with MS analysis (Fig. 3C,3D).

FETUB Restored Impaired Hormone Secretion in TP-treated KGN Cells

In order to investigate the effect of FETUB on the secretion of steroid hormones in TP-treated KGN cells, we measured the levels of hormones E_2 and P, which are closely related to ovarian function. TP treatment significantly increased the levels of E_2 and P secreted by KGN cells into the culture medium, while supplementation with FETUB significantly inhibited the levels of E_2 and P produced by TP-treated KGN cells (Fig. 4A,4B). Additionally, the change in the levels of hormones in the medium was consistent with the upregulation of *CYP11A1*, *HSD3B1*and *CYP19A1* mRNA and downregulation of *STAR* mRNA (Fig. 4C,4D).

FETUB Alleviated OS in TP-treated KGN Cells

The levels of OS biomarkers, including MDA, ROS and O_2^- were all dramatically increased after exposure to TP compared with the unexposed control group. The elevated levels of OS biomarkers could be restored by supplementing with FETUB (Fig. 4E-I). It is well established that OS results from the limited capacity of antioxidants to eliminate excessive ROS and maintain the delicate balance between the antioxidant system and the prooxidant system in cells. Following exposure to TP, the activity of antioxidant enzymes and the GSH content were all reduced in KGN cells (Fig. 4J-L). Due to its ability to increase the antioxidant capacity of KGN cells and decrease the excessive accumulation of intracellular ROS, FETUB is able to mitigate the TP-induced oxidative damage to KGN cells in this situation.

GSH Has a Critical Role in the FETUB-mediated Protection of the Secretory Function in TP-treated KGN Cells

As a key non-enzymatic antioxidant, GSH is vitally important in the body's resistance to OS. To further investigate the involvement of GSH in the protective effect of FETUB against TP-induced OS in KGN cells, the effect of the treatment with BSO (a GSH synthesis inhibitor) on TP-exposed FETUB-treated KGN cells was evaluated in this study.

As shown in Fig. 4M-N, BSO significantly inhibited the downregulation of E_2 and P levels by FETUB, suggesting that GSH is involved in the protective effect of FETUB on the secretory function of TP-exposed KGN cells. In addition, the regulatory effects of FETUB on the expression of four genes associated with steroid hormone secretion were also significantly inhibited. As shown in Fig. 4O-P, in the presence of BSO, the expression of *STAR* mRNA in KGN cells was significantly decreased, while the expression of *HSD3B1*, *CYP11A1* and *CYP19A1* mRNAs was significantly increased compared with the FETUB-treated group. These results further suggest that GSH has a key role in FETUB-mediated protection of the secretory function in TP-treated KGN cells.

FETUB Restored the Mitochondrial Functions Impaired by TP in KGN Cells

Mitochondria are recognized important organelles that regulate energy production in cells. To determine whether FETUB protects KGN cells by protecting mitochondrial function, we measured the levels of MMP, ATP, and content of mitochondrial superoxide. The flow cytometry analysis revealed that after treating KGN cells with TP for 12 hours, the proportion of cells with reduced MMP was significantly increased compared to the control group, and the red fluorescence intensity under the fluorescence microscope was significantly reduced, indicating the decline of the level of MMP (Fig. 5A,5B). Additionally, the level of ATP was markedly decreased while the level of mitochondrial superoxide was substantially increased (Fig. 5C-E). In contrast, supplementation with FETUB significantly restored the MMP and ATP levels in KGN cells and inhibited the accumulation of TP-induced mitochondrial superoxide.

FETUB Inhibits Cell Apoptosis of TP-treated in KGN Cells

Disorders of mitochondrial function are related to the activation of the mitochondrial pathway of apoptosis. We investigated the involvement of the mitochondrial apoptotic pathway in the response to treatment with TP and FETUB by measuring the expression of apoptosis-related genes and apoptosis rate in KGN cells treated with TP and FETUB. The rate of apoptosis in KGN cells was increased by TP treatment, which also caused aberrant expression of *CASP3*, *BAX*, and *BCL2* (Fig. 5F,5G). On the other hand, supplementation with FETUB reduced the rate of cell apoptosis and restored *CASP3*, *BAX*, and *BCL2* expression to normal levels. Additionally, while TP exposure increased CASP3 activity, supplementation with FETUB had the reverse effect (Fig. 5H).

FETUB Activates the TGFR2/SMAD3 Signaling Pathway in KGN Cells

It has been reported that fetuin has similar sequence homology with the TGFR2 homology 1 domain of TGF-beta Receptor and they can bind to each other in various cell lines[12, 13]. Thus, we confirmed their interaction in KGN cells by immunoprecipitation assay. Plasma membrane protein was extracted and immunoprecipitated with anti-FETUB antibody and then immunoblotted with anti-TGFR2 and anti-FETUB antibodies. The results demonstrated that FETUB and TGFR2 undoubtedly combined with one another in KGN cells. (Fig. 6A).

The SMAD3 protein is recognized as an important signal molecule that interacts with TGFR2[14]. Therefore, we investigated the possibility that SMAD3 activity might be related with the FETUB-induced signaling in KGN cells. Our results showed that TP significantly inhibited SMAD3 phosphorylation, whereas supplementation with FETUB restored SMAD3 phosphorylation in TP-treated KGN cells. Also, after pretreatment with the inhibitor SB431542 to block TGFR2, the level of SMAD3 phosphorylation decreased, indicating that FETUB has a regulatory effect on the TGFR2/SMAD3 signaling pathway (Fig. 6B,6C).

FETUB Restored the Antioxidant Capacity in TP-treated KGN Cells through a Mechanism Mediated by the TGFR2/SMAD3 Signaling Pathway

We investigated whether FETUB can regulate the TP-induced dysregulation of KGN cell function through the TGFR2/SMAD3, we conducted a series of experiments in the presence or absence of the TGFR2 inhibitor SB431542 and SMAD3 phosphorylation inhibitor SIS3, respectively. Compared with the FETUB supplementation groups, pretreatment with the inhibitors SB431542 and SIS3 significantly increased the contents of MDA, ROS and O_2^- (Fig. 7A-E). In addition, treatment of KGN cells with these inhibitors inhibited the activities of the antioxidant enzymes SOD, CAT, GPx and GR, and decreased the level of GSH, indicating that FETUB can regulate the expression of antioxidant enzymes through the TGFR2 /SMAD3 signaling pathway and then affect the level of cellular ROS, thereby ultimately regulating the cell OS response (Fig. 8F-H).

FETUB Restored the Mitochondrial Function in TP-treated KGN Cells through a Mechanism Mediated by the TGFR2/SMAD3 Signaling Pathway

Compared with the TP + FETUB group, the addition of SB431542 and SIS3 significantly reduced the FETUB supplementation-induced elevated MMP levels in TP-exposed KGN cells (Fig. 7I). In addition, treatment with SB431542 and SIS3 inhibited the FETUB-mediated decrease in KGN mitochondrial superoxide production, leading to increased superoxide levels (Fig. 7J-K). Moreover, as shown in Fig. 2.3.6E, compared with the TP + FETUB group, ATP production was significantly reduced by SB431542 and SIS3 (Fig. 7L). These results indicated that FETUB protected mitochondrial function in TP-treated KGN cells mainly by activating the TGFR2/SMAD3 signaling pathway.

FETUB Inhibited Cell Apoptosis in TP-treated KGN Cells through Activation of the TGFR2/SMAD3 Signaling Pathway

To conclusively demonstrate the protective effect of FETUB on TP-treated KGN cells through activation of the TGFR2/SMAD3 signaling pathway, we compared cell apoptosis in different groups. As shown in Fig. 8A, compared with the TP + FETUB group, the apoptosis rate in the two inhibitor groups was significantly increased. Pretreatment with the inhibitors SB431542 and SIS3 significantly inhibited the FETUB-induced changes in the expression of the *BCL2*, *BAX* and *CASP3* genes and CASP3 activity in KGN cells (Fig. 8B,8C). These results suggest that, under androgen exposure, FETUB inhibited KGN cell apoptosis by activating the TGFR2/SMAD3 signaling pathway.

FETUB restored Steroid Secretion in TP-treated KGN Cells through Activation of the TGFR2/SMAD3 Signaling Pathway

The measurement of the secretion levels of steroids (E_2 and P) in culture medium, we found that both inhibitors significantly inhibited the downregulation of E_2 and P levels induced by FETUB in TP-treated KGN cells (Fig. 8D,8E). Additionally, pretreatment with SB431542 and SIS3 in KGN cells also led to decreased expression levels of *STAR* and increased expression level of *HSD3B1*, *CYP11A1*, and *CYP19A1*, which was a restoration of the secretory function of KGN cells induced by FETUB (Fig. 8F,8G).

Discussion

PCOS is a complex endocrine disease with heterogeneous etiology, which is caused by multiple underlying pathogenesis and has different clinical manifestations. Besides the problems to control body weight, energy production, and metabolism, the mechanism also involves dysregulation of androgen, GN, and insulin secretion and activity [15–18]. The application of non-targeted high-throughput omics technologies, such as proteomics, can help us to identify candidate molecules related to the etiology of diseases, and thus to develop new therapeutic methods. There have been many proteomic studies on PCOS patients before, with a wide range of sample types, including serum, FF, GCs, ovarian tissue, and immune cells[6, 19–21]. The normal development of oocytes is inseparable from the support of GCs.

Compared with healthy women, GCs in PCOS patients may have abnormal differentiation and steroidogenesis and may respond abnormally to FSH and LH[22]. The FF is secreted by GCs and diffuses into the follicular cavity *via* capillaries and plays an important role in the physiology of follicle growth, oocyte maturation, and ovulation[23]. The chemical composition of the FF in the dominant follicle can serve as an indicator of follicular cell secretory activity and metabolism, and as a source for the identification of key proteins associated with PCOS.

The inclusion criteria of patients in previous proteomic studies on PCOS also varied from each other, including in the patient's age, BMI, regimen of ovarian hyperstimulation, and other clinical characteristics. A proteomic screen of GCs from obese subjects identified more DEPs associated with the response to impaired mitochondrial electron transport chain and endoplasmic reticulum stress, alterations that may be related to the high levels of free fatty acids detected in FF[24]. DEPs identified by proteomic analysis of serum from normal-weight adolescent women with PCOS were also shown to be enriched in GO-BP categories, such as inflammatory immune response, metabolism, and insulin-like growth factor receptor signaling[25]. Based on the characteristics of PCOS patients in our reproductive center, we set the inclusion criteria as BMI > 23.9 in order to eliminates the effect of obesity and simply focus on the effect of high androgen exposure on the protein composition of the FF.

Our study is based on the iTRAQ technique to screen for DEPs in the FF of overweight or obese women with PCOS or normal ovarian function. A total of 68 DEPs were identified after the comparison of the two groups, of which 28 DEPs showed upregulated levels in the FF, and 39 DEPs showed downregulated levels. Moreover, the functional analysis of DEPs suggested that the changes in the PCOS FF microenvironment may be related to stress, inflammation, metabolism, and other biological processes. According to our analysis of the clinical data of the 54 participants, compared with the control group, the basal blood testosterone level in the PCOS group was significantly higher, and the transferrable embryo rate was significantly lower, suggesting that PCOS patients may have lower embryo quality and adverse pregnancy ending.

Multiple studies in PCOS patients have demonstrated increased levels of inflammatory markers in the FF and plasma, increased macrophage/monocyte recruitment, and localized ovarian inflammation in these patients[26]. Transcriptomic results of GCs from PCOS patients showed increased expression levels of transcripts encoding cytokines, chemokines, and immune cell markers, and changes were more pronounced in patients with obesity or hyperandrogenism[27]. Consistent with these findings, the results of bioinformatics analysis in this study suggest that several DEPs (PXDN, QSOX1, *etc.*) in the FF play important roles in regulating IRs and ROS metabolism. PXDN is a heme-containing peroxidase that induces cell death by promoting endothelial cell apoptosis and programmed necrosis. In insulin-resistant cardiomyocytes, inhibition of PXDN can improve autophagy levels to reduce cell death by inhibiting FOXO1 expression and activity[26]. QSOX1, an enzyme responsible for oxidizing thiols during protein folding, reduces molecular oxygen to hydrogen peroxide and is associated with the disruption of intercellular contacts and cell adhesion. QSOX1 can promote the mitochondrial apoptosis pathway in hepatocellular carcinoma cells by inhibiting fatty acid and cholesterol synthesis[28].

In this study, we also identified many DEPs related to glucose metabolism and lipid metabolism. PCOS patients have a greater risk of metabolic dysfunction and are prone to complications such as diabetes and metabolic syndrome. LPL is mainly produced by adipose tissue, pancreatic islets and other tissues[29]. LPL is the rate-limiting enzyme in the hydrolysis of circulating triglyceride-rich lipoproteins, chylomicrons, and very low-density lipoproteins, and is responsible for hydrolyzing triacylglycerol-rich lipoproteins to release stored fatty acids[30]. Fibrinogen-like protein (FGL1), a novel hepatocyte cytokine that is involved in insulin resistance, has been shown to induce lipogenesis and obesity both *in vitro* and *in vivo*[31]. Insulin-like growth factor-binding protein 3 (IGFBP3) co-localizes with the retinoid X receptor-α transcription factor to maintain glucose homeostasis[32]. Elevated IGFBP3 concentration in PCOS patients with superovulation can regulate the activity of serum insulin-like growth factor, thereby promoting oocyte maturation and indicating better pregnancy outcomes[33]. Chromogranin B (CHGB) is abundantly expressed in the secretory granules of various endocrine tissues, and has the effect of regulating the production, transportation and release of secretory granules from pancreatic β-cells, and their production decreases with the destruction and exhaustion of β-cells[34, 35]. In this study, the differential expression of these proteins may be associated with PCOS, but not with obesity.

Based on the above quantitative proteomic analysis, four DEPs with significant differential expression between the two groups attracted our attention, including QSOX1, LPL, FETUB and AFM. The criteria for protein selection included the following: a threshold of fold change ≥ 1.2 between the two groups, and results of GO analysis or published literature suggesting that this protein may be involved in the pathological process of PCOS[15, 30, 36]. For the above four DEPs, we performed targeted ELISA measurement of their protein concentrations in the FF of 18 additional cases in each group. The results revealed that compared with the CON group, the expression levels of FETUB and LPL in the FF of the PCOS group were significantly higher, while the levels of QSOX1 and AFM were markedly reduced in the group of PCOS patients, which are consistent with the results of proteomics, thus further confirming the reliability of the proteomic analysis.

FETUB is a member of the fetuin protein family that forms part of the cystatin protein superfamily, and is associated with several important biological processes including infertility, metabolism, and liver disease. FETUB mRNA levels were found to be downregulated in the acute phase of inflammation in rats, indicating that it may be engaged in the recovery phase of inflammation[10]. However, the changes in its acute-phase levels were significantly different among different species. Both iTRAQ quantitative proteomics analysis and its verification results revealed that the secretion of FETUB in the FF of PCOS patients was significantly higher compared with the control group, suggesting that it may act as a positive acute phase response protein in humans, but its function and mechanism in PCOS is unclear.

Hyperandrogenemia has been recognized as an important factor in exacerbating reproductive-related clinical symptoms of PCOS and promoting the development of metabolic diseases. Hyperandrogenism is both the most important cause of PCOS and a contributing factor in the development of the disease. Excessive androgens can result in the destruction of GCs and alter the follicular microenvironment, leading to follicular atresia in PCOS. There are five types of androgens in women:

dehydroepiandrosterone sulfate (DHEAS), dehydroepiandrosterone (DHEA), androstenedione (A_4), testosterone (T), and dihydrotestosterone (DHT). In serum, the concentrations of these five androgens in the order from high to low are DHEAS, DHEA, A_4, T, and DHT, but their biological activities are in the opposite order. Pre-experiments were conducted in the early stage of this study to explore the dysfunction of KGN cells due to various androgen stimulation. Among them, TP exhibited the most significant effect. Various studies have shown that TP has a similar effect to that of testosterone in animals but with longer effect time, thus it is widely used in the establishment of PCOS models[16, 37, 38].

Accordingly, we used TP to mimics the hyperandrogenic environment of PCOS in KGN cells. As the main steroid hormones secreted by the ovary, E_2 and P were significantly increased in the medium after TP treatment, suggesting that TP treatment effectively caused the dysfunction of ovarian-related steroid hormone secretion. Supplementation with FETUB significantly inhibited the TP-induced increase of E_2 and P in the medium, showing a certain therapeutic effect.

Abnormal secretion of steroid hormones may be related to several key enzymes in the process of hormone synthesis. *STAR* is the most critical rate-limiting enzyme in the entire steroid hormone synthesis process. In addition, 3βHSD is responsible for converting DHEA to A_4 and can also convert pregnenolone to P. Additionally, A_4 can be converted to testosterone and estrone by cytochrome P450aro in GCs. Subsequently, testosterone is converted to E_2 by the P450arom in GCs[39–41]. Therefore, we analyzed the mRNA expression levels of genes encoding these enzymes. This analysis revealed that the mRNA expression of *STAR* was decreased, while the mRNA expressions of *CYP11A1*, *HSD3B1* and *CYP19A1* were increased. The alterations in the expression of these genes may be involved in the disorder of KGN hormone secretion caused by androgen. Indeed, the increased expression of *CYP11A1* and *HSD3B1* may explain the increased level of P after TP treatment. A possible reason for the increase of the *CYP19A1* gene expression is that the abnormal increase of androgens triggers the body's own regulatory mechanism, and by increasing the expression of the *CYP19A1* gene, the excess androgen is converted into E_2 [42].

Several studies have reported that OS is closely related to the pathogenesis of PCOS. OS is the result of an imbalance between free radical production and antioxidant defense. There is evidence that OS can induce or exacerbate the main symptoms of PCOS. TNF can stimulate the *in vitro* proliferation of rat membrane cells which are responsible for synthesis of androgen[43]. Also, the androgen level of rat membrane cells can be upregulated by pro-inflammatory factors, and the antioxidant resveratrol can inhibit androgen production by reducing the level of CYP17A1 mRNA[44]. In addition, the pro-oxidative effects of androgens *in vivo* and *in vitro* have been confirmed, as a result hyperandrogenism of PCOS patients aggravated by OS will cause further ROS production, creating a vicious circle[15]. Despite the fact that ROS induces the dominant follicle to complete meiosis I, the subsequent maturation of the dominant follicle is inseparable from antioxidants, and GSH plays an important role in inhibiting the pro-apoptotic effect of ROS[37]. Increased ROS in cumulus cells is associated with changes in the tricarboxylic acid cycle and nicotinamide-adenosine-dinucleotide catabolism in the FF of PCOS patients.

Excessive OS may be associated with the poor pregnancy rate and high miscarriage rate of PCOS women[16].

The detection of OS and antioxidant biomarkers is often necessary when it comes to assessing the risk of oxidative damage. ROS is a class of molecules produced by aerobic biological oxygen metabolism and is the most important product of OS imbalance. ROS can function as second messengers to participate in proliferation, differentiation, or apoptosis of cells[5]. MDA, one of the final products of lipid peroxidation, was found to be markedly increased in the FF and serum of PCOS patients, and thus can be used as a biomarker reflecting the degree of lipid peroxidation in PCOS patients[45, 46].

At the same time, GSH and the antioxidant enzymes SOD, CAT, GPx and GR can inactivate or stabilize free radicals before they damage cells to maintain the cellular redox balance. GSH is one of the most indispensable non-enzymatic antioxidants. In addition to its role in the antioxidant defense system, GSH is also responsible for the detoxification of exogenous substances, amino acid transport and other biological processes[47]. SOD, CAT, GPx, and GR are major members of the enzymatic antioxidant defense systems, whose role is to scavenge free radicals and nascent oxygen.

Numerous studies have found that OS dysfunction in PCOS patients is independent of factors, such as obesity and IR but may be associated with hyperandrogenemia[48]. The degree of OS in PCOS is positively correlated with androgen levels, and antioxidant therapy can effectively improve the OS status in PCOS patients and reduce androgen levels to a certain extent. In this study, the changes in the contents of the OS biomarkers ROS, O_2^-, MDA and GSH and the decrease in antioxidant enzyme activities consistently indicated that OS was induced in TP-treated KGN cells. Supplementation with FETUB can increase the GSH content and reduce the OS level in KGN cells by downregulating the levels of ROS, O_2^- and MDA, and simultaneously enhance the antioxidant defense ability of KGN cells by increasing the enzymatic activities of four antioxidant enzymes. Clinical studies have shown that OS may further exacerbate the disorder of glucose and lipid metabolism and sex hormone metabolism in PCOS patients. To further elucidate the regulatory mechanism of FETUB, we selected the GSH inhibitor BSO for further investigation. The results indicated that BSO could significantly inhibit the protective effect of FETUB on the secretion of steroid hormones.

Since genome-wide association studies and other studies of the nuclear genome have failed to give any clues about the precise mechanisms of PCOS pathogenesis, considerable attention has now been shifted to mitochondria[17]. There are increasing reports that hyperandrogenemia interacts with mitochondrial dysfunction, which may be a potential contributor to PCOS disease[49]. Androgen exposure induces excessive ROS production, which in turn leads to IR. Islets from rats treated with DHT had lower mtDNA copy numbers, lower oxygen consumption rates, and lower ATP levels compared to controls[50]. Mitochondria as the major organelles for intracellular energy production play an important role in maintaining cellular energy balance[51]. Our study showed that mitochondrial dysfunction in TP-treated KGN cells manifested as a significant decrease in the MMP, an increase in mitochondrial superoxide content, and a decrease in ATP production; while treatment with FETUB could significantly restore the

MMP and ATP levels and reduce mitochondrial superoxide levels, suggesting that FETUB protects mitochondrial function in TP-treated KGN cells.

Apoptosis of GCs is well-known to be closely related to the development of PCOS, and the cell death and proliferation rates of the GC population in PCOS patients are significantly different from those in the non-PCOS population[52]. Apoptosis is an underlying mechanism of follicular atresia and underlies the cyclical growth and degeneration of follicles in the human ovary[53]. Atresia of mature late preantral and antral follicles is dominated by apoptosis of ovarian GCs[54]. Abnormal apoptosis of GCs not only affects the maturation of oocytes, but also affects the process of converting testosterone into E_2, resulting in excessive androgen accumulation, while hyperandrogenism can cause follicle development arrest in PCOS patients, creating a vicious circle[55].

As a group of mutually antagonistic proteins, *BCL2* and *BAX* are engaged in mitochondrial apoptotic pathway [56]. The upregulation of the BCL2 family of pro-apoptotic factors can activate the mitochondrial apoptotic pathway mediated by the caspase family of apoptotic proteases by increasing mitochondrial permeability and promoting the release of apoptotic factors from mitochondria into the cytoplasm. CASP3 is functionally essential for the induction of apoptosis in GCs during follicular atresia[57]. Various apoptotic protein inhibitors block mammalian GCs apoptosis by inhibiting CASP3 activity [58]. Under normal circumstances, CASP3 exists as an inactive precursor, and is activated only when stimulated by certain apoptotic factors.

In this study, after induction with TP, the apoptosis level of KGN cells was significantly increased, while the expression of the anti-apoptotic factor BCL2 was inhibited, the expression of the pro-apoptotic factor *BAX* was increased, and the expression and enzyme activity of CASP3 were significantly increased. Compared with the TP-treated group, the apoptosis rate of KGN cells supplemented with FETUB was significantly decreased. The above results suggest that the apoptosis rate of KGN cells after TP treatment is increased. Supplementation with FETUB can inhibit apoptotic factors and activate anti-apoptotic factors, reduce the apoptosis rate of GCs, and ultimately play a protective effect on the cells.

FETUA and FETUB are two glycoproteins from the fetuin family containing two tandem cystatin domains and found in high concentrations in serum[59]. FETUA is one of the acute phase proteins produced in the liver. and may act as anti-inflammatory protein in injury-induced inflammatory responses[60, 61]. FETUB, like FETUA, is also mainly synthesized in the liver[13]. Normally, it is detected at relatively low levels in other secretory tissues[59, 62]. Based on the structural similarity between FETUB and FETUA, researchers have proposed that FETUB may have a wider range of biological functions[63]. However, the precise mechanism by which FETUB regulates GCs in PCOS remains unclear.

TGFR2 homology 1 domain shares similar sequences with FETUB[13]. It is well-known that numerous biological processes, such as cell apoptosis and proliferation, stem cell differentiation, migration, and homeostasis are triggered by TGFR2 activation[64]. Indeed, it has been reported that FETUB bound with TGFR2 on the vascular smooth muscle cell (VSMC) membrane, and supplementation with FETUB

activated the phosphorylation of SMAD3 in VSMCs, and the phosphorylation of SMAD3 could be inhibited by SB431542, a selective inhibitor of TGFR2[12]. Our immunoprecipitation results also showed that FETUB interacted with TGFR2 on the membrane of KGN cells. These results suggest that FETUB may engage in interactions with TGFR2 and regulate the downstream signaling.

The TGF-β receptor family is crucial for the development of embryo, extracellular matrix, and bone remodeling. of the members of this family act by binding receptors for the regulation of cell signaling pathways. The receptors found in the cell membrane are mainly divided into three categories, of which type II receptors are serine/threonine and tyrosine kinase receptors. When the ligand binds to the receptor, after first binding to the type II receptor, the receptor recruits the type I receptor and phosphorylates it in the membrane, and then phosphorylates the downstream SMAD molecule. Different receptor combinations can diversely activate different downstream SMADs. For instance, ALK4, ALK5 and ALK7 act as type I receptors to activate the signaling molecule SMAD3. SMAD3 is a key signaling molecule in the response to TGFR2 in cells[14]. To verify the regulatory role of the TGFR2 /SMAD3 signaling pathway in the FETUB-induced antioxidant process, we used SB431542, a specific inhibitor of TGFR. This inhibitor is a specific inhibitor of the cell membrane surface receptors ALK4, ALK5 and ALK7, which can effectively block the signaling pathway triggered by TGFB in cells[65]. In this study, we found that FETUB could activate TGFR-related signaling in KGN cells, whereas SB431542 inhibited the activation of SMAD3 phosphorylation in cells due to the binding of FETUB to TGFR.

The results of SMAD activation are affected by various factors, such as its target genes, related transcription factors, and cell states. Therefore, SMADs have a wide range of regulatory effects, and sometimes produce diametrically opposite effects in different cellular physiological states[66]. For example, different phosphorylated forms of SMAD3 show differences in regulating liver cancer progression. More specifically, liver cancer can be prevented by phosphorylation of the -COOH terminus of SMAD3 but promoted by phosphorylation of the linker region of SMAD3[67]. There are also many conflicting reports on the role of the TGF-β/SMAD3 signaling pathway in the regulation of OS. Some studies suggest that the activation of SMAD3 induces OS in various diseases and is involved in the apoptosis process of various tissues[68, 69]. However, in adult mice, activation of TGF-βI/SMAD3 signaling in the hippocampus by inflammatory stimuli was significantly reduced[67]. It has been reported by Ding *et al*. that BMP combined with endothelial regulators protected neurons by activating the SMAD3-Akt-NRF2 pathway and inhibited neuroinflammation in a mouse model of cerebral ischemia, thereby reducing ischemic brain injury[70].

On this basis, we separately pretreated KGN cells with the TGF-βR inhibitor SB431542 and SMAD3 phosphorylation inhibitor SIS3 and measured the level of OS, mitochondrial function, apoptosis, and steroid secretion in KGN cells. The data indicated that the treatment with the two specific inhibitors effectively inhibited the antioxidant effect of the recombinant FETUB protein, which manifested as disordered cellular steroid secretion, aggravated OS damage, mitochondrial function damage, and exacerbated apoptosis. Our study implies that SMAD3 may be the target of FETUB under TP-induced OS.

Phosphorylation of SMAD3 by FETUB may cause the activation of other antioxidant signaling pathways, thereby exerting its protective effect on TP-treated KGN cells.

Conclusion

In this study, FETUB was found from the screening of FF samples, and the its regulatory effect and mechanism on KGN cells under high androgen environment were first clarified *in vitro*. In conclusion, our study found that FETUB alleviates OS and mitochondrial dysfunction induced by TP in KGN cells by upregulating the TGFR2/SMAD3 signaling pathway, which provided theoretical basis and data support for the treatment of PCOS (Fig. 9).

Abbreviations

PCOS: Polycystic ovary syndrome; FETUB: Fetuin-B; DEPs: Differentially expressed proteins; FF: Follicular fluid; TP: Testosterone propionate; OS: Oxidative stress; TGFR2: Transforming growth factor beta receptor 2; GN: Gonadotropin; GCs: Granulosa cells; FETUA: Fetuin A; IR: Insulin resistance; CON: Control; ELISA: Enzyme-linked immunosorbent assay; ART: Assisted reproductive treatment; LPL: Lipoprotein lipase; QSOX1: Quiescin sulfhydryl oxidase 1; AFM: Afamin; MDA: Malondialdehyde; GSH: Reduced glutathione; SOD: Superoxide dismutase; CAT: Catalase; GPx: Glutathione peroxidase; GR: Glutathione reductase; TMRE: Tetramethylrhodamine ethyl ester; E_2: Estradiol; P: Progesterone; qRT-PCR: Quantitative reverse transcription-polymerase chain reaction; *GAPDH*: Glyceraldehyde-3-phosphate dehydrogenase; IP: Immunoprecipitation; BMI: Body-mass index; FSH: Follicle-stimulating hormone; GO: Gene ontology; BP: Biological process; CC: Cellular component; MF: Molecular function; COG: Clusters of orthologous groups; KEGG: Kyoto encyclopedia of genes and genomes; MMP: Mitochondrial membrane potential

Declarations

Ethics approval and consent to participate

The study was conducted according to the guidelines of the Declaration of Helsinki and approved by ethics committee of Second Hospital of Jilin University (No.122 of 2020). Each patient/subject signed an informed consent prior to sample collection.

Consent for publication

Not applicable.

Competing interests

The authors declare that they have no competing interests.

Availability of data and materials

The mass spectrometry proteomics data have been deposited to the ProteomeXchange Consortium via the PRIDE partner repository with the dataset identifier PXD036531[71]. Here is the reviewer account details. Username: reviewer_pxd036531@ebi.ac.uk

Password: 2N8YFJUA

Funding

The author(s) disclosed receipt of the following financial support for the research, authorship, and/or publication of this article: Funding for this work was provided by the Natural Science Foundation of Jilin Province, China (YDZJ202201ZYTS084).

Authors' Contributions

All of the authors contributed to the conception of the article. YG and GW performed collection of FF samples and subjects' information. YG and LZ performed proteomics data analysis. YG and YM performed experiment *in vitro*. Conception and design of this project were performed by YG and YZ. The first draft of the manuscript was prepared by YG. GW and LZ performed subsequent amendments. YZ revised the manuscript. All authors read and approved the submitted version final manuscript.

Acknowledgements

The authors would like to thank Wuhan GeneCreate Biological Engineering Co., Ltd for performing the proteomic analysis.

References

1. Carmina E, Lobo RA: **Polycystic ovary syndrome (PCOS): arguably the most common endocrinopathy is associated with significant morbidity in women**. J Clin Endocrinol Metab 1999, **84**:1897–1899.
2. Asunción M, Calvo RM, San Millán JL, Sancho J, Avila S, Escobar-Morreale HF: **A prospective study of the prevalence of the polycystic ovary syndrome in unselected Caucasian women from Spain**. J Clin Endocrinol Metab 2000, **85**:2434–2438.
3. Diamanti-Kandarakis E, Dunaif A: **Insulin resistance and the polycystic ovary syndrome revisited: an update on mechanisms and implications**. Endocr Rev 2012, **33**:981–1030.
4. Kaya C, Erkan AF, Cengiz SD, Dünder I, Demirel ÖE, Bilgihan A: **Advanced oxidation protein products are increased in women with polycystic ovary syndrome: relationship with traditional and nontraditional cardiovascular risk factors in patients with polycystic ovary syndrome**. Fertil Steril 2009, **92**:1372–1377.
5. Mohammadi M: **Oxidative Stress and Polycystic Ovary Syndrome: A Brief Review**. Int J Prev Med 2019, **10**:86.
6. Ambekar AS, Kelkar DS, Pinto SM, Sharma R, Hinduja I, Zaveri K, Pandey A, Prasad TS, Gowda H, Mukherjee S: **Proteomics of follicular fluid from women with polycystic ovary syndrome suggests**

molecular defects in follicular development. J Clin Endocrinol Metab 2015, **100**:744–753.

7. Pal D, Dasgupta S, Kundu R, Maitra S, Das G, Mukhopadhyay S, Ray S, Majumdar SS, Bhattacharya S: **Fetuin-A acts as an endogenous ligand of TLR4 to promote lipid-induced insulin resistance**. Nat Med 2012, **18**:1279–1285.
8. Meex RC, Hoy AJ, Morris A, Brown RD, Lo JC, Burke M, Goode RJ, Kingwell BA, Kraakman MJ, Febbraio MA, Greve JW, Rensen SS, Molloy MP, Lancaster GI, Bruce CR, Watt MJ: **Fetuin B Is a Secreted Hepatocyte Factor Linking Steatosis to Impaired Glucose Metabolism**. Cell Metab 2015, **22**:1078–1089.
9. Mokou M, Yang S, Zhan B, Geng S, Li K, Yang M, Yang G, Deng W, Liu H, Liu D, Zhu Z, Li L: **Elevated Circulating Fetuin-B Levels Are Associated with Insulin Resistance and Reduced by GLP-1RA in Newly Diagnosed PCOS Women**. Mediators Inflamm 2020, **2020**:2483435.
10. Olivier E, Soury E, Ruminy P, Husson A, Parmentier F, Daveau M, Salier JP: **Fetuin-B, a second member of the fetuin family in mammals**. Biochem J 2000, **350 Pt 2**:589–597.
11. Livak KJ, Schmittgen TD. Analysis of relative gene expression data using real-time quantitative PCR and. (1046–2023 (Print)).
12. Jung SH, Lee D, Jin H, Lee HM, Ko HM, Lee KJ, Kim SJ, Ryu Y, Choi WS, Kim B, Won KJ: **Fetuin-B regulates vascular plaque rupture via TGF-β receptor-mediated Smad pathway in vascular smooth muscle cells**. Pflugers Arch 2020, **472**:571–581.
13. Demetriou M, Binkert C, Sukhu B, Tenenbaum HC, Dennis JW: **Fetuin/alpha2-HS glycoprotein is a transforming growth factor-beta type II receptor mimic and cytokine antagonist**. J Biol Chem 1996, **271**:12755–12761.
14. Heldin CH, Miyazono K, ten Dijke P: **TGF-beta signalling from cell membrane to nucleus through SMAD proteins**. Nature 1997, **390**:465–471.
15. Mancini A, Bruno C, Vergani E, d'Abate C, Giacchi E, Silvestrini A: **Oxidative Stress and Low-Grade Inflammation in Polycystic Ovary Syndrome: Controversies and New Insights**. Int J Mol Sci 2021, **22**:
16. Özer A, Bakacak M, Kıran H, Ercan Ö, Köstü B, Kanat-Pektaş M, Kılınç M, Aslan F: **Increased oxidative stress is associated with insulin resistance and infertility in polycystic ovary syndrome**. Ginekol Pol 2016, **87**:733–738.
17. Shukla P, Mukherjee S: **Mitochondrial dysfunction: An emerging link in the pathophysiology of polycystic ovary syndrome**. Mitochondrion 2020, **52**:24–39.
18. Zhang Y, Zhao W, Xu H, Hu M, Guo X, Jia W, Liu G, Li J, Cui P, Lager S, Sferruzzi-Perri AN, Li W, Wu XK, Han Y, Brännström M, Shao LR, Billig H: **Hyperandrogenism and insulin resistance-induced fetal loss: evidence for placental mitochondrial abnormalities and elevated reactive oxygen species production in pregnant rats that mimic the clinical features of polycystic ovary syndrome**. J Physiol 2019, **597**:3927–3950.
19. Ahmed M, Neville MJ, Edelmann MJ, Kessler BM, Karpe F: **Proteomic analysis of human adipose tissue after rosiglitazone treatment shows coordinated changes to promote glucose uptake**. Obesity (Silver Spring) 2010, **18**:27–34.

20. Yu Y, Tan P, Zhuang Z, Wang Z, Zhu L, Qiu R, Xu H: **DIA proteomics analysis through serum profiles reveals the significant proteins as candidate biomarkers in women with PCOS**. BMC Med Genomics 2021, **14**:125.
21. Zhang X, Xu X, Li P, Zhou F, Kong L, Qiu J, Yuan Z, Tan J: **TMT Based Proteomic Analysis of Human Follicular Fluid From Overweight/Obese and Normal-Weight Patients With Polycystic Ovary Syndrome**. Front Endocrinol (Lausanne) 2019, **10**:821.
22. Franks S, Mason H, Willis D: **Follicular dynamics in the polycystic ovary syndrome**. Mol Cell Endocrinol 2000, **163**:49–52.
23. Fortune JE: **Ovarian follicular growth and development in mammals**. Biol Reprod 1994, **50**:225–232.
24. Si C, Wang N, Wang M, Liu Y, Niu Z, Ding Z: **TMT-based proteomic and bioinformatic analyses of human granulosa cells from obese and normal-weight female subjects**. Reprod Biol Endocrinol 2021, **19**:75.
25. Manousopoulou A, Al-Daghri NM, Sabico S, Garay-Baquero DJ, Teng J, Alenad A, Alokail MS, Athanasopoulos N, Deligeoroglou E, Chrousos GP, Bacopoulou F, Garbis SD: **Polycystic Ovary Syndrome and Insulin Physiology: An Observational Quantitative Serum Proteomics Study in Adolescent, Normal-Weight Females**. Proteomics Clin Appl 2019, **13**:e1800184.
26. Lima P, Nivet AL, Wang Q, Chen YA, Leader A, Cheung A, Tzeng CR, Tsang BK: **Polycystic ovary syndrome: possible involvement of androgen-induced, chemerin-mediated ovarian recruitment of monocytes/macrophages**. Biol Reprod 2018, **99**:838–852.
27. Adams J, Liu Z, Ren YA, Wun WS, Zhou W, Kenigsberg S, Librach C, Valdes C, Gibbons W, Richards J: **Enhanced Inflammatory Transcriptome in the Granulosa Cells of Women With Polycystic Ovarian Syndrome**. J Clin Endocrinol Metab 2016, **101**:3459–3468.
28. Lake DF, Faigel DO: **The emerging role of QSOX1 in cancer**. Antioxid Redox Signal 2014, **21**:485–496.
29. Wang H, Eckel RH: **Lipoprotein lipase: from gene to obesity**. Am J Physiol Endocrinol Metab 2009, **297**:E271-288.
30. Olivecrona G: **Role of lipoprotein lipase in lipid metabolism**. Curr Opin Lipidol 2016, **27**:233–241.
31. Wu HT, Chen SC, Fan KC, Kuo CH, Lin SY, Wang SH, Chang CJ, Li HY: **Targeting fibrinogen-like protein 1 is a novel therapeutic strategy to combat obesity**. FASEB J 2020, **34**:2958–2967.
32. Liu B, Lee HY, Weinzimer SA, Powell DR, Clifford JL, Kurie JM, Cohen P: **Direct functional interactions between insulin-like growth factor-binding protein-3 and retinoid X receptor-alpha regulate transcriptional signaling and apoptosis**. J Biol Chem 2000, **275**:33607–33613.
33. Schoyer KD, Liu HC, Witkin S, Rosenwaks Z, Spandorfer SD: **Serum insulin-like growth factor I (IGF-I) and IGF-binding protein 3 (IGFBP-3) in IVF patients with polycystic ovary syndrome: correlations with outcome**. Fertil Steril 2007, **88**:139–144.
34. Bearrows SC, Bauchle CJ, Becker M, Haldeman JM, Swaminathan S, Stephens SB: **Chromogranin B regulates early-stage insulin granule trafficking from the Golgi in pancreatic islet β-cells**. J Cell Sci 2019, **132**:

35. Herold Z, Herold M, Rosta K, Doleschall M, Somogyi A: **Lower serum chromogranin B level is associated with type 1 diabetes and with type 2 diabetes patients with intensive conservative insulin treatment**. Diabetol Metab Syndr 2020, **12**:61.
36. Xue S, Han H, Rui S, Yang M, Huang Y, Zhan B, Geng S, Liu H, Chen C, Yang G, Li L: **Serum Fetuin-B Levels Are Elevated in Women with Metabolic Syndrome and Associated with Increased Oxidative Stress**. Oxid Med Cell Longev 2021, **2021**:6657658.
37. Tsai-Turton M, Luong BT, Tan Y, Luderer U: **Cyclophosphamide-induced apoptosis in COV434 human granulosa cells involves oxidative stress and glutathione depletion**. Toxicol Sci 2007, **98**:216–230.
38. Gaweł S, Wardas M, Niedworok E, Wardas P: **[Malondialdehyde (MDA) as a lipid peroxidation marker]**. Wiad Lek 2004, **57**:453–455.
39. Bloom MS, Mok-Lin E, Fujimoto VY: **Bisphenol A and ovarian steroidogenesis**. Fertil Steril 2016, **106**:857–863.
40. Manna PR, Dyson MT, Stocco DM: **Regulation of the steroidogenic acute regulatory protein gene expression: present and future perspectives**. Mol Hum Reprod 2009, **15**:321–333.
41. Miller WL, Auchus RJ: **The molecular biology, biochemistry, and physiology of human steroidogenesis and its disorders**. Endocr Rev 2011, **32**:81–151.
42. Luo M, Zheng LW, Wang YS, Huang JC, Yang ZQ, Yue ZP, Guo B: **Genistein exhibits therapeutic potential for PCOS mice via the ER-Nrf2-Foxo1-ROS pathway**. Food Funct 2021, **12**:8800–8811.
43. Rzepczynska IJ, Foyouzi N, Piotrowski PC, Celik-Ozenci C, Cress A, Duleba AJ: **Antioxidants induce apoptosis of rat ovarian theca-interstitial cells**. Biol Reprod 2011, **84**:162–166.
44. Ortega I, Villanueva JA, Wong DH, Cress AB, Sokalska A, Stanley SD, Duleba AJ: **Resveratrol potentiates effects of simvastatin on inhibition of rat ovarian theca-interstitial cells steroidogenesis**. J Ovarian Res 2014, **7**:21.
45. Artimani T, Karimi J, Mehdizadeh M, Yavangi M, Khanlarzadeh E, Ghorbani M, Asadi S, Kheiripour N: **Evaluation of pro-oxidant-antioxidant balance (PAB) and its association with inflammatory cytokines in polycystic ovary syndrome (PCOS)**. Gynecol Endocrinol 2018, **34**:148–152.
46. Isık H, Aynıoglu O, Tımur H, Sahbaz A, Harma M, Can M, Guven B, Alptekin H, Kokturk F: **Is Xanthine oxidase activity in polycystic ovary syndrome associated with inflammatory and cardiovascular risk factors**. J Reprod Immunol 2016, **116**:98–103.
47. Aydin M, Dirik Y, Demir C, Tolunay HE, Demir H: **Can we reduce oxidative stress with liver transplantation**. J Med Biochem 2021, **40**:351–357.
48. Savić-Radojević A, Mažibrada I, Djukić T, Stanković ZB, Plješa-Ercegovac M, Sedlecky K, Bjekić-Macut J, Simić T, Mastorakos G, Macut D: **Glutathione S-transferase (GST) polymorphism could be an early marker in the development of polycystic ovary syndrome (PCOS) - an insight from non-obese and non-insulin resistant adolescents**. Endokrynol Pol 2018, **69**:366–374.
49. Dabravolski SA, Nikiforov NG, Eid AH, Nedosugova LV, Starodubova AV, Popkova TV, Bezsonov EE, Orekhov AN: **Mitochondrial Dysfunction and Chronic Inflammation in Polycystic Ovary Syndrome**. Int J Mol Sci 2021, **22**:

50. Attardi G, Schatz G: **Biogenesis of mitochondria**. Annu Rev Cell Biol 1988, **4**:289–333.
51. Toleikis A, Trumbeckaite S, Liobikas J, Pauziene N, Kursvietiene L, Kopustinskiene DM: **Fatty Acid Oxidation and Mitochondrial Morphology Changes as Key Modulators of the Affinity for ADP in Rat Heart Mitochondria**. Cells 2020, **9**:
52. Das M, Djahanbakhch O, Hacihanefioglu B, Saridogan E, Ikram M, Ghali L, Raveendran M, Storey A: **Granulosa cell survival and proliferation are altered in polycystic ovary syndrome**. J Clin Endocrinol Metab 2008, **93**:881–887.
53. Tilly JL: **Apoptosis and ovarian function**. Rev Reprod 1996, **1**:162–172.
54. Morita Y, Tilly JL: **Oocyte apoptosis: like sand through an hourglass**. Dev Biol 1999, **213**:1–17.
55. Dell'Aquila ME, Albrizio M, Maritato F, Minoia P, Hinrichs K: **Meiotic competence of equine oocytes and pronucleus formation after intracytoplasmic sperm injection (ICSI) as related to granulosa cell apoptosis**. Biol Reprod 2003, **68**:2065–2072.
56. Tilly JL, Tilly KI, Kenton ML, Johnson AL: **Expression of members of the bcl-2 gene family in the immature rat ovary: equine chorionic gonadotropin-mediated inhibition of granulosa cell apoptosis is associated with decreased bax and constitutive bcl-2 and bcl-xlong messenger ribonucleic acid levels**. Endocrinology 1995, **136**:232–241.
57. Matikainen T, Perez GI, Zheng TS, Kluzak TR, Rueda BR, Flavell RA, Tilly JL: **Caspase-3 gene knockout defines cell lineage specificity for programmed cell death signaling in the ovary**. Endocrinology 2001, **142**:2468–2480.
58. Johnson AL, Langer JS, Bridgham JT: **Survivin as a cell cycle-related and antiapoptotic protein in granulosa cells**. Endocrinology 2002, **143**:3405–3413.
59. Lee C, Bongcam-Rudloff E, Sollner C, Jahnen-Dechent W, Claesson-Welsh L: **Type 3 cystatins; fetuins, kininogen and histidine-rich glycoprotein**. Front Biosci (Landmark Ed) 2009, **14**:2911–2922.
60. Lim P, Moutereau S, Simon T, Gallet R, Probst V, Ferrieres J, Gueret P, Danchin N: **Usefulness of fetuin-A and C-reactive protein concentrations for prediction of outcome in acute coronary syndromes (from the French Registry of Acute ST-Elevation Non-ST-Elevation Myocardial Infarction [FAST-MI])**. Am J Cardiol 2013, **111**:31–37.
61. Weikert C, Stefan N, Schulze MB, Pischon T, Berger K, Joost HG, Häring HU, Boeing H, Fritsche A: **Plasma fetuin-a levels and the risk of myocardial infarction and ischemic stroke**. Circulation 2008, **118**:2555–2562.
62. Denecke B, Gräber S, Schäfer C, Heiss A, Wöltje M, Jahnen-Dechent W: **Tissue distribution and activity testing suggest a similar but not identical function of fetuin-B and fetuin-A**. Biochem J 2003, **376**:135–145.
63. Jahnen-Dechent W, Schinke T, Trindl A, Müller-Esterl W, Sablitzky F, Kaiser S, Blessing M: **Cloning and targeted deletion of the mouse fetuin gene**. J Biol Chem 1997, **272**:31496–31503.
64. Gambineri A, Pelusi C, Vicennati V, Pagotto U, Pasquali R: **Obesity and the polycystic ovary syndrome**. Int J Obes Relat Metab Disord 2002, **26**:883–896.

65. Schaub JR, Huppert KA, Kurial S, Hsu BY, Cast AE, Donnelly B, Karns RA, Chen F, Rezvani M, Luu HY, Mattis AN, Rougemont AL, Rosenthal P, Huppert SS, Willenbring H: **De novo formation of the biliary system by TGFβ-mediated hepatocyte transdifferentiation**. Nature 2018, **557**:247–251.
66. Morikawa M, Derynck R, Miyazono K: **TGF-β and the TGF-β Family: Context-Dependent Roles in Cell and Tissue Physiology**. Cold Spring Harb Perspect Biol 2016, **8**:
67. Zhang C, Li L, Hou S, Shi Z, Xu W, Wang Q, He Y, Gong Y, Fang Z, Yang Y: **Astragaloside IV inhibits hepatocellular carcinoma by continually suppressing the development of fibrosis and regulating pSmad3C/3L and Nrf2/HO-1 pathways**. J Ethnopharmacol 2021, **279**:114350.
68. Tang H, L Kennedy C, Lee M, Gao Y, Xia H, Olguin F, Fraga DA, Ayers K, Choi S, Kim M, Tehrani A, Sowb YA, Rando TA, Shrager JB: **Smad3 initiates oxidative stress and proteolysis that underlies diaphragm dysfunction during mechanical ventilation**. Sci Rep 2017, **7**:14530.
69. Lv Y, Han X, Yao Q, Zhang K, Zheng L, Hong W, Xing X: **1α,25-dihydroxyvitamin D3 attenuates oxidative stress-induced damage in human trabecular meshwork cells by inhibiting TGFβ-SMAD3-VDR pathway**. Biochem Biophys Res Commun 2019, **516**:75–81.
70. Ding P, Chen W, Yan X, Zhang J, Li C, Zhang G, Wang Y, Li Y: **BMPER alleviates ischemic brain injury by protecting neurons and inhibiting neuroinflammation via Smad3-Akt-Nrf2 pathway**. CNS Neurosci Ther 2021,
71. Perez-Riverol Y, Bai J, Bandla C, García-Seisdedos D, Hewapathirana S, Kamatchinathan S, Kundu DJ, Prakash A, Frericks-Zipper A, Eisenacher M, Walzer M, Wang S, Brazma A, Vizcaíno JA. The PRIDE database resources in 2022: a hub for mass spectrometry-based. (1362–4962 (Electronic)).

Figures

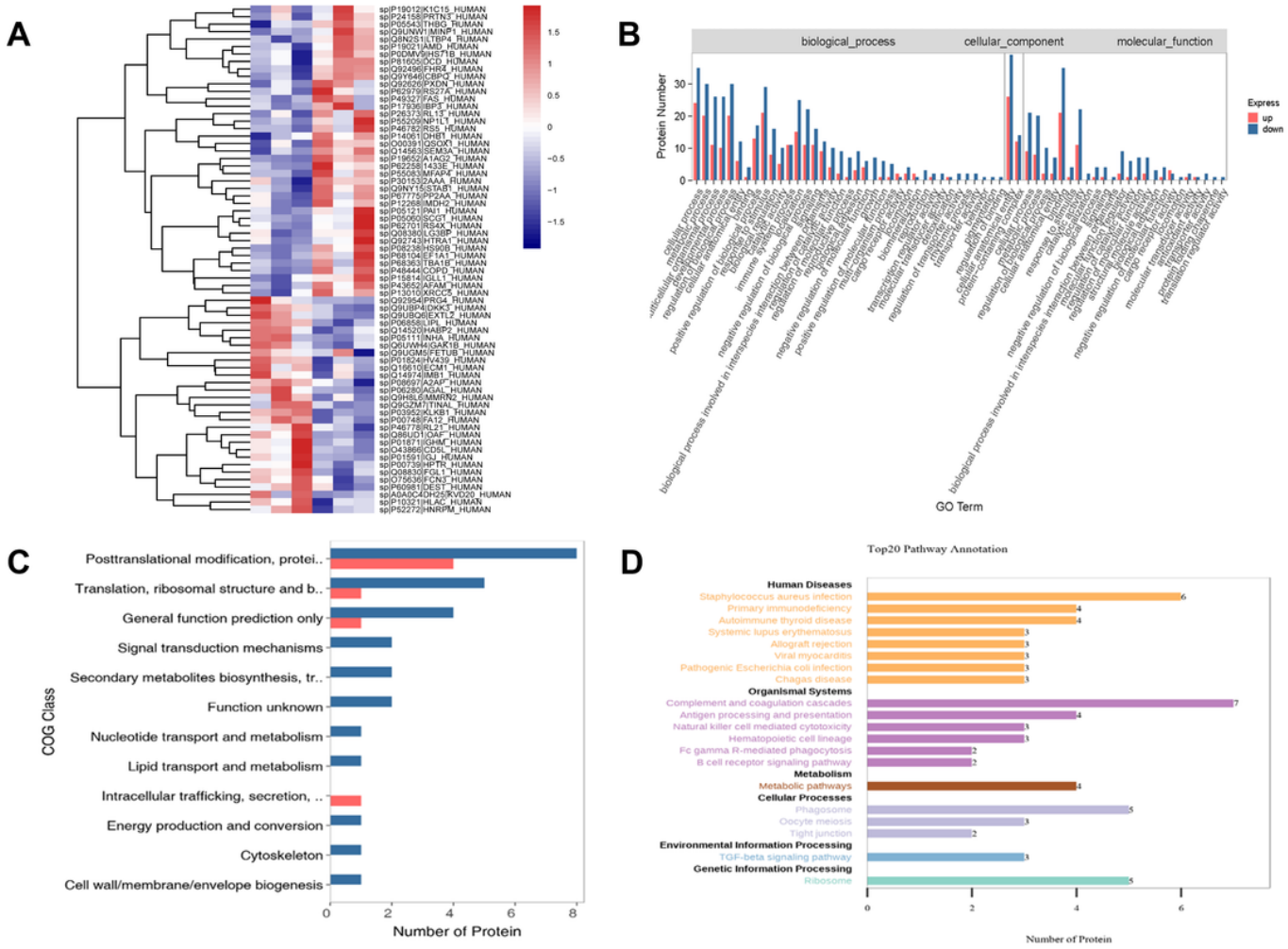

Figure 1

Results of iTRAQ based proteomic analysis and bioinformatics analysis **(A)**Hierarchical clustering heatmaps of DEPs in PCOS group. **(B)** GO classification annotation histogram of DEPs in PCOS group. **(C)** COG Classification Annotation Bar Chart of DEPs in PCOS group. **(D)** Pathway Classification Annotation Bar Chart of DEPs in PCOS group.

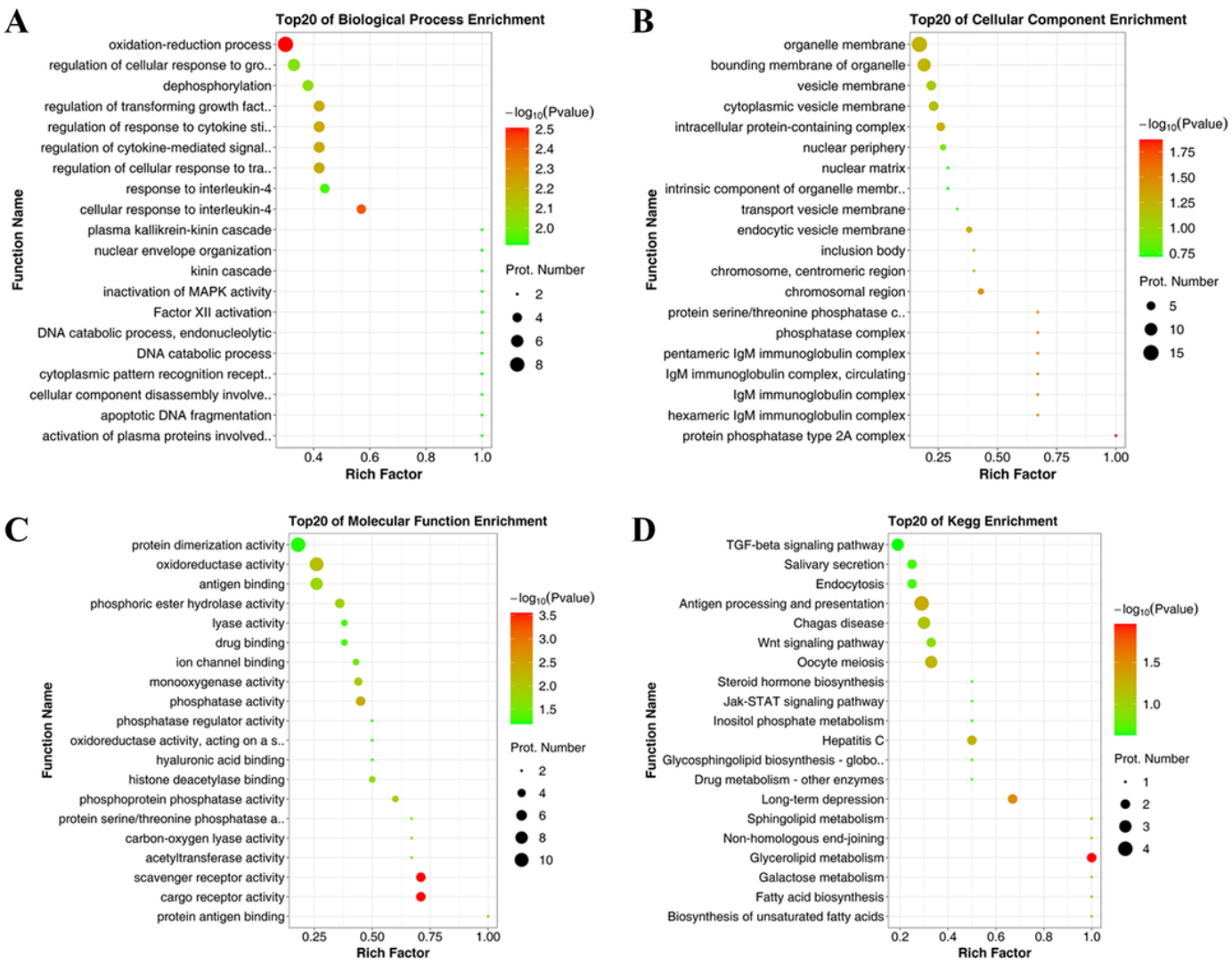

Figure 2

Enrichment Analysis Bubble Plot of DEPs in PCOS group **(A)** GO-enriched biological process analysis. **(B)** GO-enriched cellular component analysis. **(C)**GO-enriched molecular function analysis. **(D)** KEGG pathway enrichment analysis.

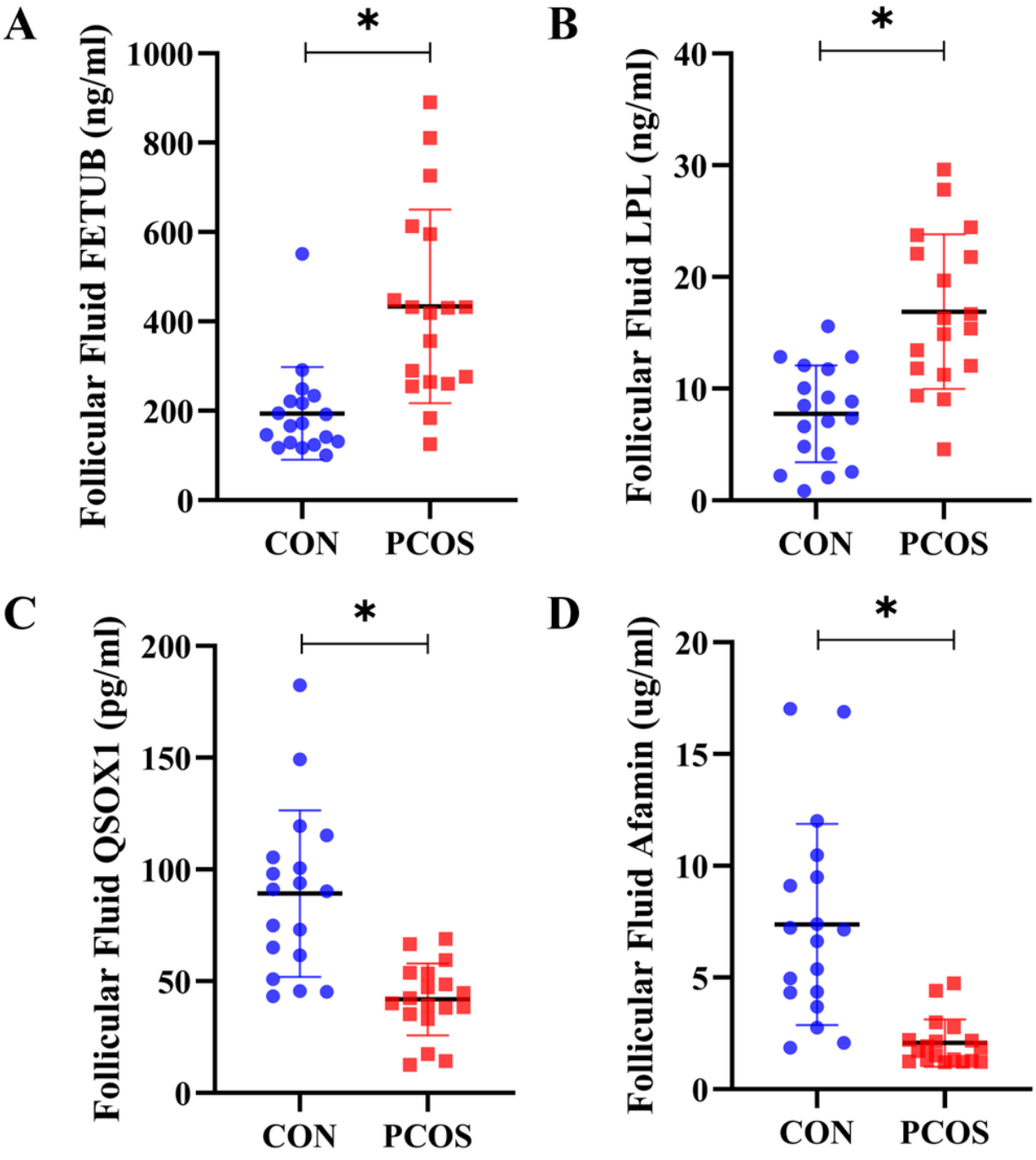

Figure 3

ELISA verification of four DEPs in FF samples of CON group and PCOS group **(A)**FETUB **(B)** LPL **(C)** QSOX1 **(D)** Afamin. *P<0.05.

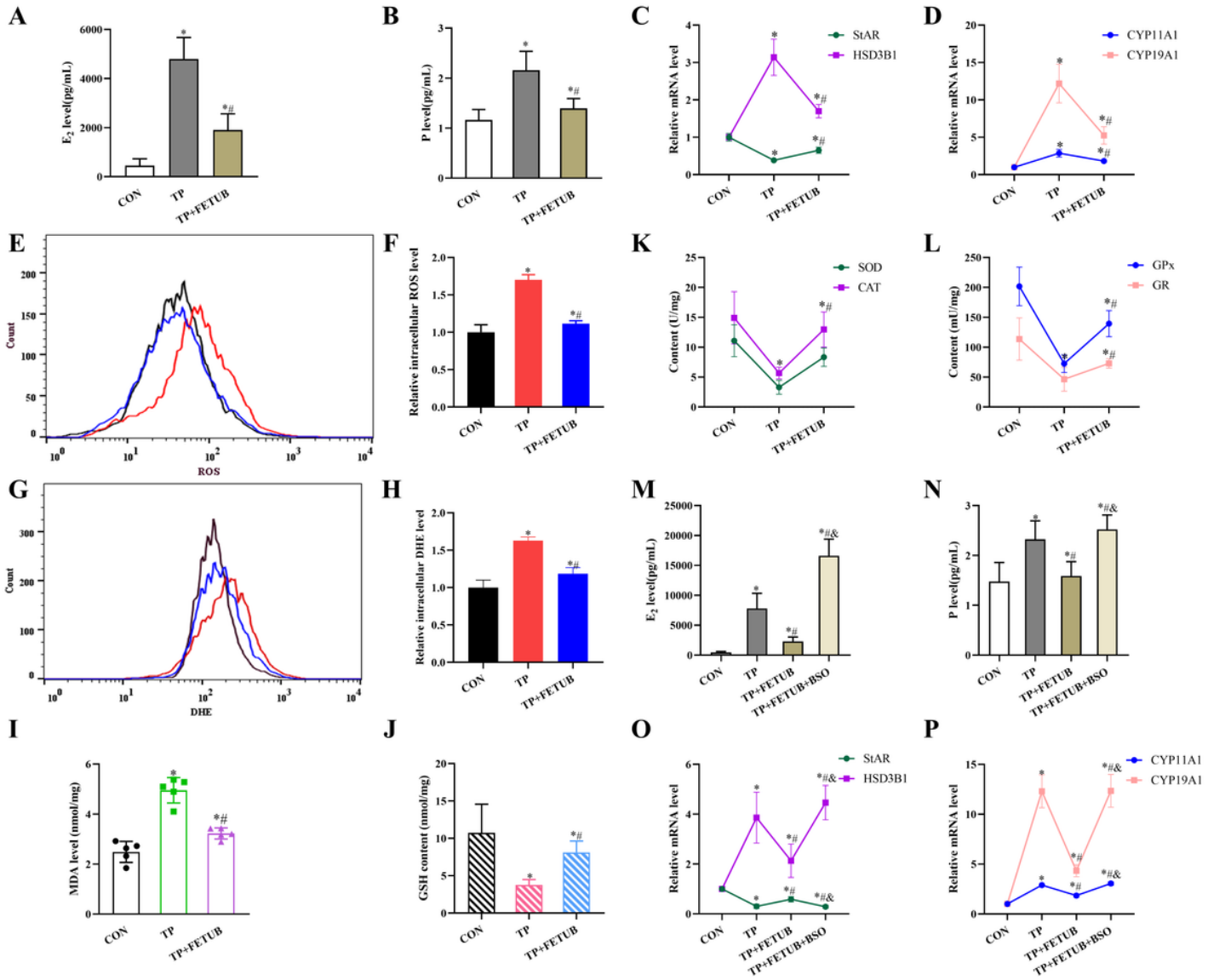

Figure 4

The protective effects of FETUB on hormone secretion and anti-oxidation in TP-treated KGN cells **(A-B)** FETUB restored elevated levels of E2and P in TP-treated KGNs. **(C-D)** FETUB restored impaired hormone secretion in TP-treated KGN cells by upregulating *CYP11A1*, *HSD3B1*and *CYP19A1* mRNA and downregulating *STAR* mRNA. **(E-I)** FETUB restored elevated levels of OS biomarkers including ROS, O2- and MDA in TP-treated KGNs. **(J-L)** FETUB restored activity of antioxidant enzymes and content of GSH in TP-treated KGNs. **(M-P)** BSO significantly inhibited the downregulation of E2 and P levels by FETUB with the upregulation of *CYP19A1*, *CYP11A1* and *HSD3B1* and the downregulation of *STAR*. Data represent mean ± standard error, **P* < 0.05, *#*P* < 0.05.

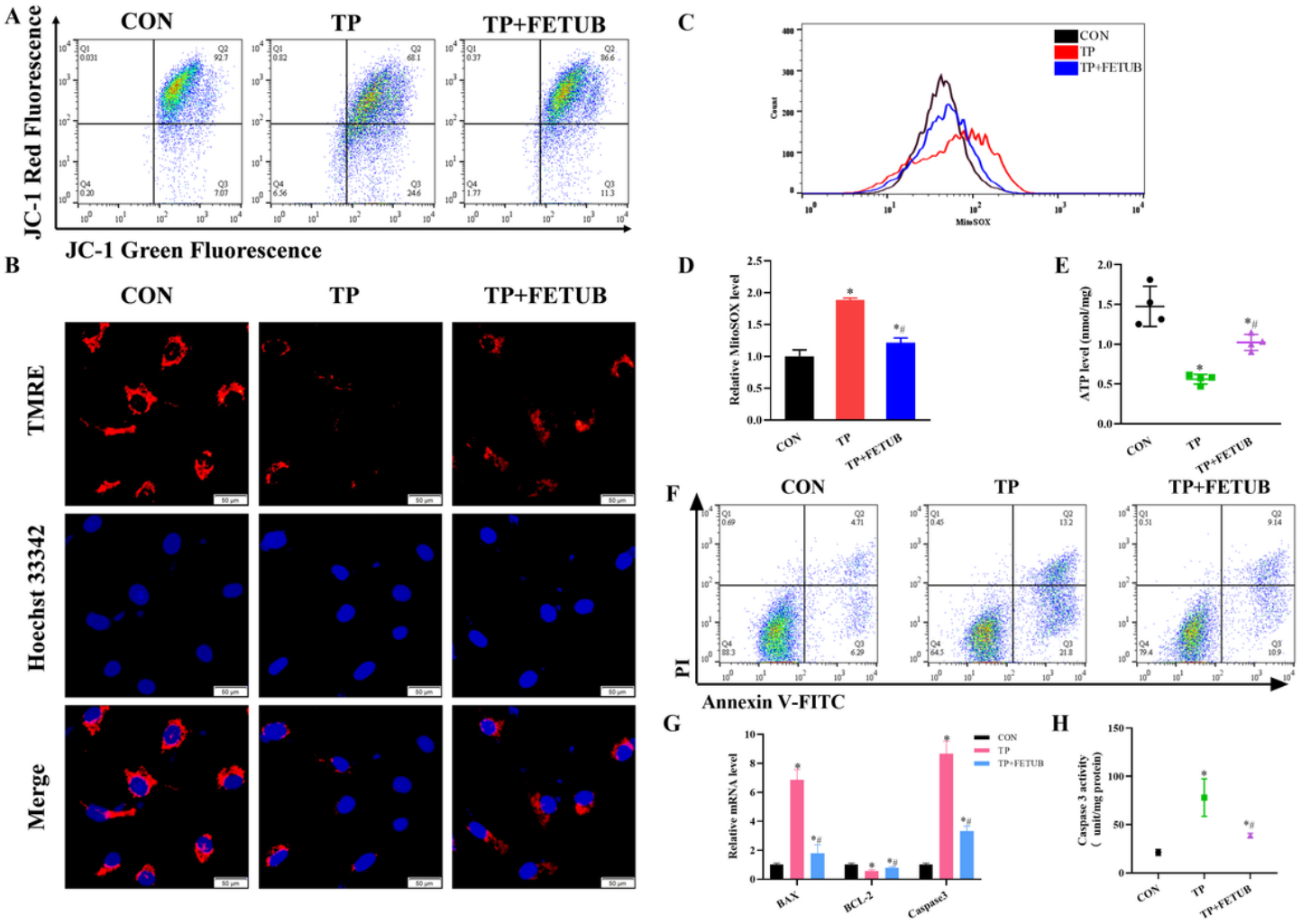

Figure 5

The protective effects of FETUB on mitochondrial function and cell apoptosis in TP-treated KGN cells **(A-B)** FETUB restored mitochondrial membrane potential in TP-treated KGNs. **(C-D)** FETUB reduced content of mitochondrial superoxide in TP-treated KGNs. **(E)** FETUB restored the ATP level in TP-treated KGNs. **(F-H)** FETUB inhibited apoptosis of TP-treated KGNs with the upregulation of *BCL2*, downregulation of *CASP3* and *BAX*and increase of CASP3 activity. Data represent mean ± standard error, **P*< 0.05, *#*P* < 0.05. Bar = 50μm.

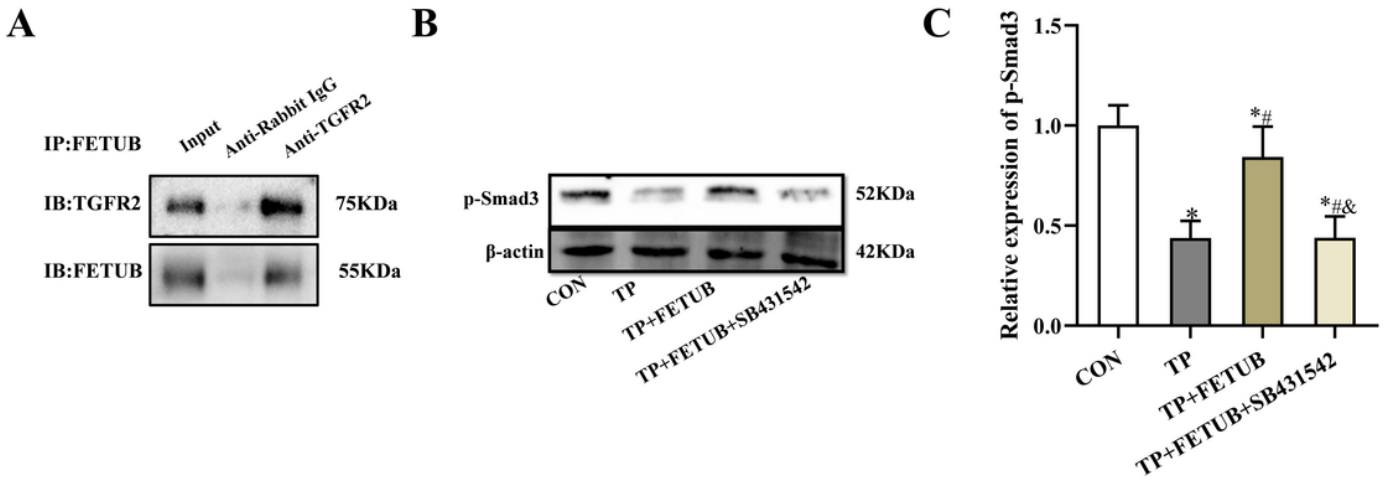

Figure 6

(A) Binding of FETUB and TGFR2 protein in KGN cells. Membrane proteins were immunoprecipitated with anti-fetuin-B antibody and then immunoblotted with anti-TGFR2 and anti-fetuin-B antibodies. IP, immunoprecipitation. IB, immunoblot. **(B-C)** FETUB enhanced the phosphorylation of SMAD3 in TP-treated KGN cells which could be inhibited by SB431542. Data represent mean ± standard error, **P* < 0.05.

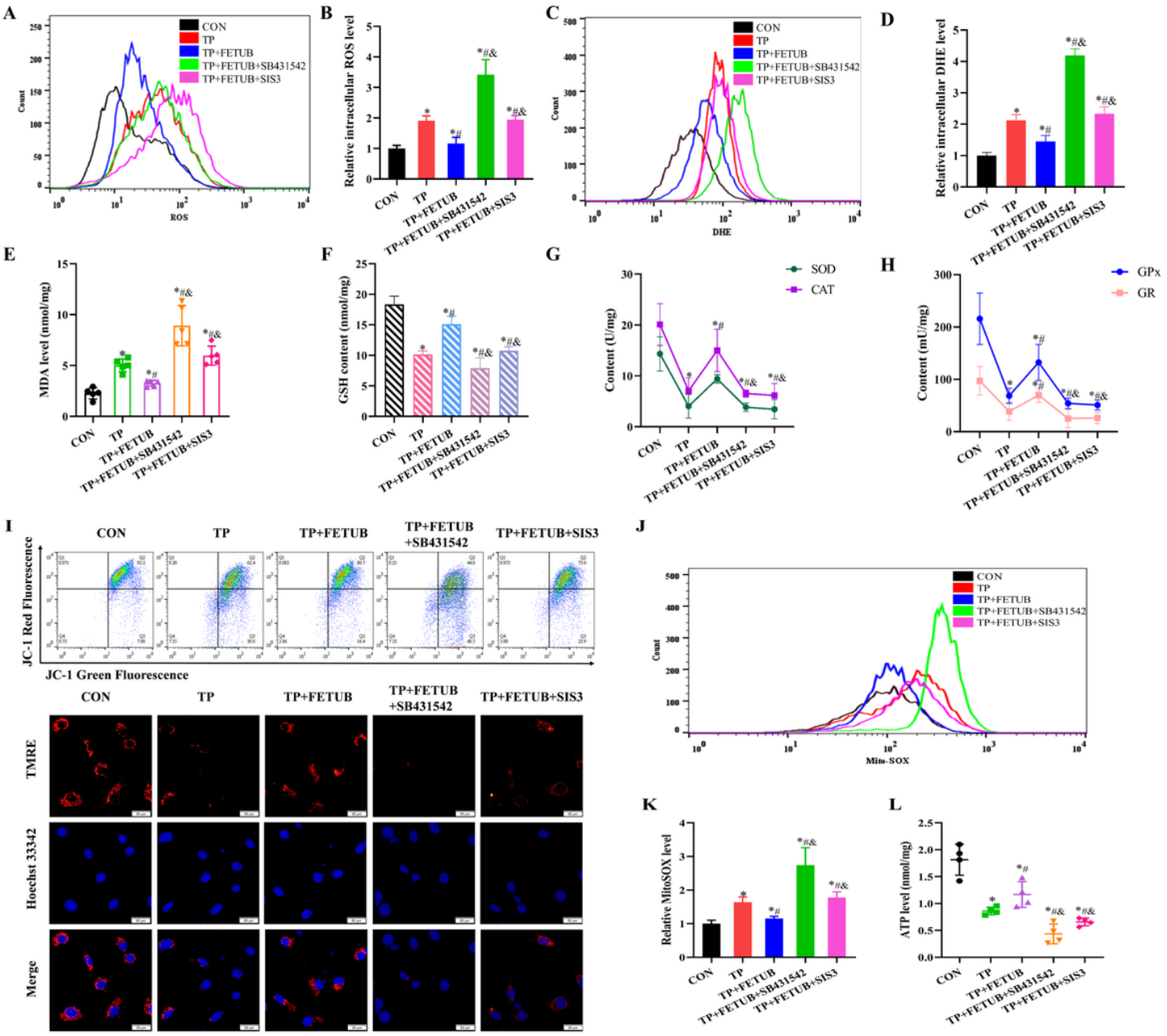

Figure 7

(A-E) Pretreatment with the inhibitors SB431542 and SIS3 significantly increased the contents of MDA, ROS and O2-in TP-treated KGN cells. **(F-H)** Pretreatment with the inhibitors SB431542 and SIS3 inhibited the activities of antioxidant enzymes and decreased content of GSH in TP-treated KGN cells. **(I)** Pretreatment with the inhibitors SB431542 and SIS3 reduced the MMP levels in TP-treated KGN cells. **(J-L)**Pretreatment with the inhibitors SB431542 and SIS3 increased the level of mitochondrial superoxide and reduced the ATP production. Data represent mean ± standard error, *$P < 0.05$, *#$P < 0.05$, *#&$P < 0.05$. Bar = 50μm.

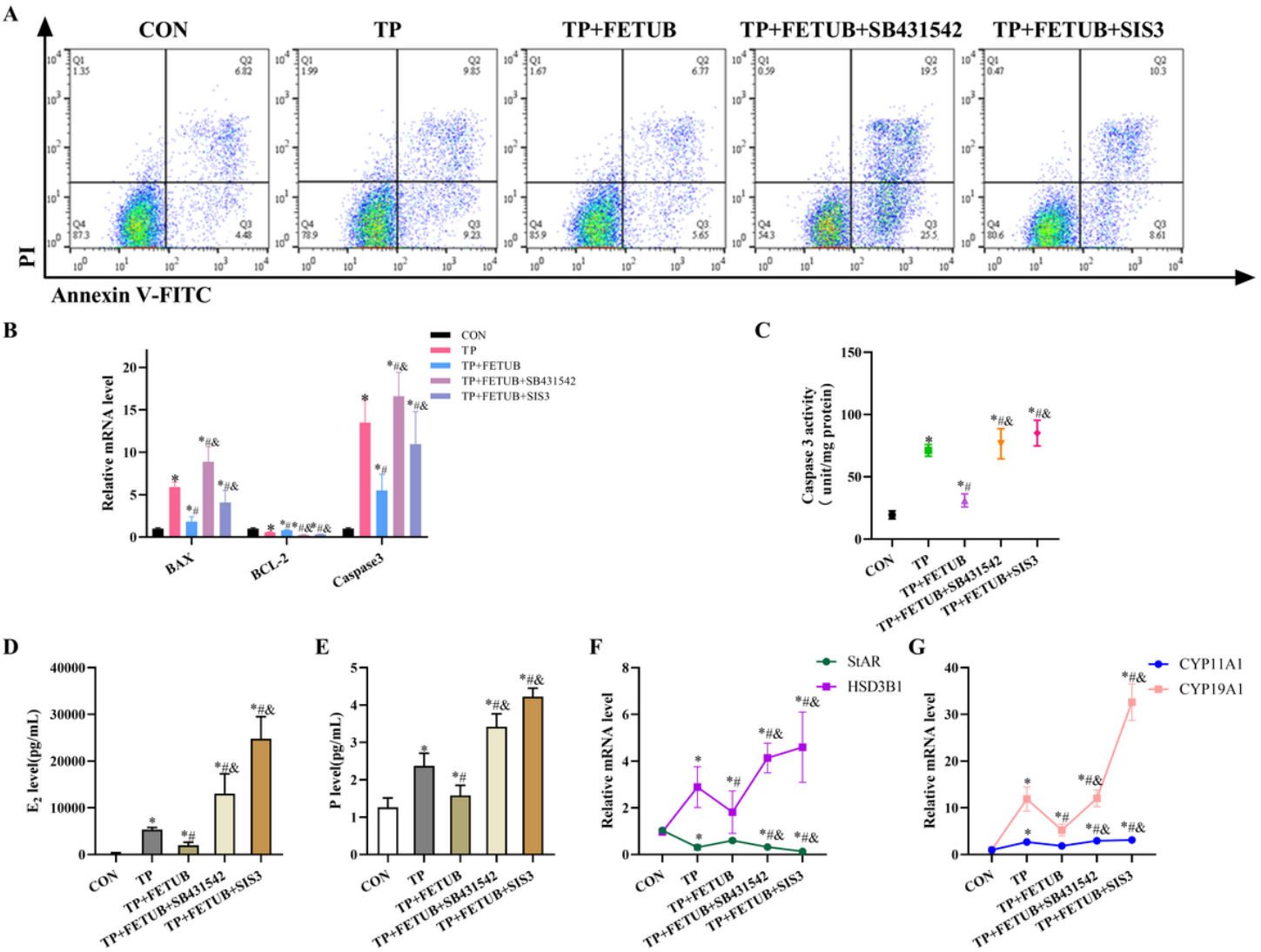

Figure 8

(A) Pretreatment with the inhibitors SB431542 and SIS3 increased the rate of apoptosis of TP-treated KGN cells.**(B-C)** The expression of apoptosis related gene and activity of Caspase 3 in TP-treated KGN cells was changed after treatment with SB431542 and SIS3. **(D-G)**Pretreatment of the inhibitors SB431542 and SIS3 exacerbated the disturbance of hormone secretion by increasing the level of E2 and P with the change of associated genes expression. Data represent mean ± standard error, *P< 0.05, *#P < 0.05, *#&P < 0.05.

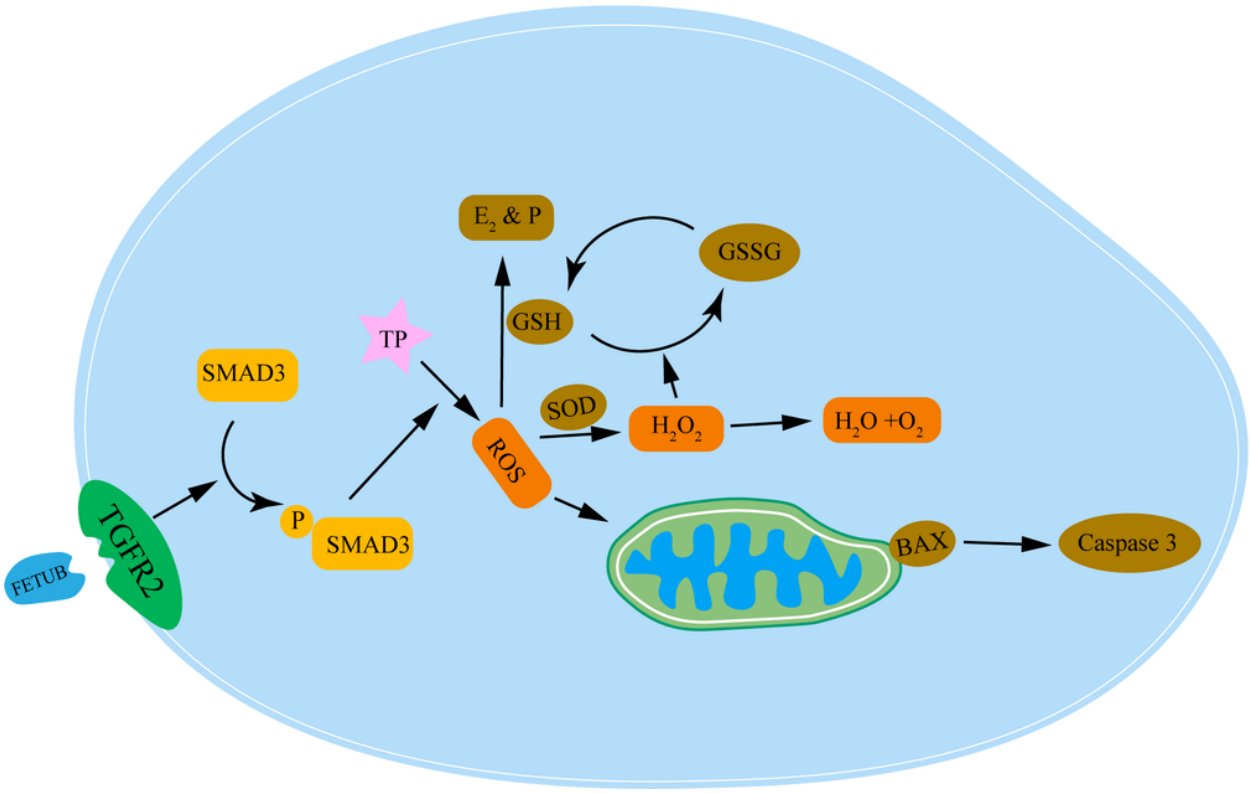

Figure 9

Schematic summarizing the effect and mechanism of FETUB alleviating TP-induced oxidative stress in KGN cells. Supplementation of FETUB reversed the disturbance of hormone secretion caused by TP, reduced OS damage, repaired mitochondrial function, and reduced the level of cell apoptosis through binding to TGF-β receptor and activating SMAD3 phosphorylation.

Supplementary Files

This is a list of supplementary files associated with this preprint. Click to download.

- supplementaryfigure1.tif
- supplementaryfigure2.tif
- supplementaryfigure3.tif
- supplementaryfigure4.tif
- supplementaryfigurelegends.docx